62-1556

NEWS OF SCHOOLS OF HIGHER EDUCATION,
ELECTROMECHANICS
(SELECTED ARTICLES)

295 802

UNEDITED ROUGH DRAFT TRANSLATION

NEWS OF SCHOOLS OF HIGHER EDUCATION, ELECTROMECHANICS
(SELECTED ARTICLES)

English Pages: 79

SOURCE: Russian periodical, Izvestiya Vysshykh Uchebnykh Zavedeniy, Elektormekhanika, Nr. 2, 1962, pp. 140-154, 155-167, 177-188, 189-195.

SOV/144-62-0-2-4/7, 5/7, 6/7, 7/7

PREPARED BY:

TRANSLATION SERVICES BRANCH
FOREIGN TECHNOLOGY DIVISION
WP-AFB, OHIO.

TABLE OF CONTENTS

CALCULATION OF THE CHARACTERISTICS OF SYMMETRICAL-PULSE INDUCTION GENERATORS

A. N. Tkachenko

Calculation of the electrical characteristics of symmetrical-pulse induction generators (SPIG's), which are now being widely used as power supplies for electronic-pulse machines, is an important element of their design.

Below we give the methods and basic relationships which allow us to calculate the basic characteristics of SPIG's for a steady-state operational regime.

Without dwelling on the well-known SPIG design [1, 2], we note merely that it is similar to the design of ordinary induction machines with semi-enclosed stator grooves and differs only in the way in which the toothed zone is made. Here the width of the tooth of the rotor (inductor) of the SPIG is considerably narrower (or considerably wider) than the width of the toothed division of the stator. The magnetic system of the SPIG may be of like or opposite poles; however, the former possesses a number of advantages over the latter (greater efficiency, lower inductance in the stator winding, etc.),

as a result of which the like-pole version may be regarded as the main one. Accordingly, the following study applies mainly to the like-pole version, although the basic results obtained may also be used for the calculation of opposite-pole generators.

For the investigation we shall assume at the outset that the permeability of steel does not depend on the magnitude of the magnetic-field strength (and induction), i.e., μ_{st} = const, and we shall disregard the influence of hysteresis. These assumptions may be justified by the fact that the saturation of the magnetic circuit of a SPIG (and in particular of the toothed zone) is usually slight, and the ferromagnetic regions of this circuit are made of materials with narrow hysteresis loops.

We shall approximately calculate the influence of eddy currents which arise from loading the machine (mainly within the massive sections of the magnetic circuit) by introducing into our discussion certain damping windings located on the stator and rotor concentric to the shaft of the machine (similar to the field winding) and distributed in a definite manner over the length of the machine.

Under the assumptions made, the flux within the machine may be considered to be the result of the superposition of the flux produced by the stator, field and damping windings. The flux produced by the current i_s in the stator may be represented as the sum of two groups of currents, of which one is coupled with the end parts of the stator winding and the other with the conductors of the winding in their slotted parts. The total flux of the first group will be called the longitudinal flux (Φ_d), while that of the second group will be called the transverse flux (Φ_q).

Figure 1 shows schematically a part of the toothed zone and a

simplified picture of the magnetic field of the stator. The magnetic lines of the excitation flux (Φ_e) are also shown.

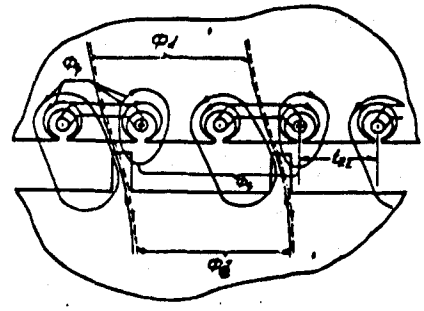

Fig. 1. Simplified picture of the magnetic field in the toothed zone of a SPIG.

As a result of the magnetic coupling which exists between all the windings under consideration, currents arise in the winding, when the machine is loaded. Therefore, taking into consideration the assumptions made above, the resultant (total) interlinkage of the stator windings (ψ_p) may be represented in the form

$$\psi_p = L_q i_s + L_d i_s + M_{sd_1} i_{d_1} + M_{sd_2} i_{d_2} + M_{sf} i_f, \qquad (1)$$

where L_q and L_d = the transverse and longitudinal self-inductance of the stator winding, respectively. (These correspond to the transverse and longitudinal interlinkage of the stator winding);

M_{sd_1} and M_{sd_2} = the mutual inductance of the stator winding and each of the damping windings;

i_{d_1} and i_{d_2} = the damping winding currents;

M_{sf} = the mutual inductance of the stator and field coils;

i_f = the current in the field coil with the machine loaded.

The transverse flux of the stator winding does not form a magnetic coupling with the other windings.

The longitudinal flux of the stator winding may be represented as the sum of two components, one of which is coupled only with the stator winding, closes around the end parts, and passes through the charged core of the stator, the air, and partly through the teeth of the rotor, while the other is coupled with the damping and field windings and closes along the basic magnetic circuit (stator teeth, air gap, rotor teeth, rotor casing, core, and stator casing). The longitudinal self-inductance corresponding to the first part of the longitudinal interlinkage of the stator winding is denoted by L_{ds}, while that of the second part is denoted by L_{dm}. The total longitudinal self-inductance is obviously

$$L_d = L_{ds} + L_{dm}. \qquad (2)$$

The current in the field winding of a loaded machine under the steady-state regime of operation may be represented as the sum of two components, one of which, i_{fo}, is a direct current, which arises in the circuit under the action of a constant voltage applied to the field circuit, while the other, i_{fd}, is an alternating current, which arises in the field winding as a consequence of its magnetic coupling with the stator winding and damping windings. Thus, the current in the field winding is

$$i_f = i_{fo} + i_{fd}. \qquad (3)$$

Substituting (2) and (3) in (1), after proper grouping, we obtain

$$\psi_p = (L_q + L_{aa})i_a + M_{af}i_{fo} + [L_{dm}i_a + M_{ad}i_{d_1} + M_{ad}i_{d_2} + M_{af}i_{fd}]. \qquad (4)$$

At a sufficiently high variation frequency the alternating magnetic

fluxes are almost completely damped in the massive parts of the magnetic circuit. Therefore the term in brackets on the right-hand side of (4) may be neglected.

A more detailed analysis indicated that the self-inductance, $L_q + L_{ds}$, is a periodic function of time and contains, in the general case, a constant component (L_o) and even and odd harmonics. However, the induction pulsations are insignificant and may be neglected.

Taking the latter into account, the expression for the resultant interlinkage of the stator winding may be approximately written in the form

$$\psi_p = L_o i_s + M_{sf} i_{fo} \qquad (4a)$$

The mutual inductance M_{sf} of generators of symmetrical pulses is a periodic function of time, the variable component of which contains only odd harmonics. After differentiating the right- and left-hand sides of (4a) we obtain an expression for the instantaneous value of the resultant emf of the stator winding in the form

$$e_p = -\frac{d\psi_p}{dt} = -L_o\frac{di_s}{dt} - i_{fo}\frac{dM_{sf}}{dt}. \qquad (5)$$

The resultant emf must be balanced by the sum of the voltage at the terminals of the stator (U_s) and the voltage drop over the resistance of the stator winding (r_s). Taking into account that the term $(-i_{fo}\frac{dM_{sf}}{dt})$ in (5) is none other than the open-circuit emf, e_o (the emf for an open stator winding), we obtain the basic differential equation of a SPIG stator circuit in the form

$$e_o = r_s i_s + L_o\frac{di_s}{dt} + U_s. \qquad (6)$$

It should be emphasized that differential equation (6) is valid not only for SPIG's in the steady-state regime but also when a disturbance arises in the stator circuit.

Under real conditions, the regime of operation of a SPIG on an active load is the main one; therefore the main load tests of these generators are conducted on linear active loads. For the conditions indicated differential equation (6) assumes the form

$$e_o = Ri_s + L_o \frac{di_s}{dt}, \qquad (6a)$$

where $R = r_s + R_1$ is the active resistance of the stator circuit, while R_1 is the resistance of the load.

The solution of differential equation (6a) for the steady-state regime may be obtained, as is known, either in the form of a Fourier series or in closed form. The solution in the form of a series may prove to be convenient for the calculation of the effective values of the current and voltage and of the static characteristics relating these quantities. The closed form of the solution is convenient for determining the shape of the current and voltage curves and also for calculating the average values of these quantities. When the curve of the open-circuit emf is given graphically, a solution in closed form may be obtained graphically for the current [3]. It may also be obtained analytically, if the analytical expression for the function of the emf, $e_o = e_o(t)$, is known [4, 5].

The open-circuit emf of a SPIG is a complex periodic function of time, the analytical expression for which within the limits of a period (half-period) may be given by piecewise-continuous functions. In this case the solution of (6a) for every interval has the form

$$i_{\text{в}} = e^{-p(t-t_1)} \int \frac{e_{o1}(t-t_1)}{L_o} e^{p(t-t_1)} dt \cdot G_1 e^{-p(t-t_1)}, \qquad (7)$$

where $\rho = \frac{R}{L_o}$

t_l = the moment in time corresponding to the start of the l-th interval;

$e_{ol}(t-t_l)$ = a function of the open-circuit emf during the l-th interval ($t_l < t < t_{l+1}$);

C_l = a constant of integration determined from the time-boundary conditions. The time boundary conditions result, in turn, from the conditions of continuity of the current function.

The emf curve of a coil may be obtained as the difference between the two identical emf's of the conductors which form the sides of the coil. Here it must be kept in mind that the emf's of the conductors are displaced with respect to each other by a half-period. The shape of the emf of the conductor is similar to the shape of the curve of the field distribution in the air gap, a curve which is moving relative to the conductors together with the rotor. The curve of the field distribution in the air gap may be calculated according to the well-known formula of R. Richter, which has been converted and simplified by I. S. Rogachev [1,6].

The instantaneous value of the emf of the entire stator winding may be obtained as the product of the emf of one coil times the number of coils connected in series in the winding.

An analogous expression for the open-circuit emf of a SPIG may be obtained, for example, with the aid of a three-piece approximation of the half-wave emf by functions of the form:

for the first interval ($0 < t < t_1$)

$$e_{01} = U_1 = E_1 \frac{e^{\alpha\omega t} - 1}{e^{\alpha\omega t_1} - 1};$$

for the second interval ($t_1 < t < t_2$)

$$e_{02} = U_2 = E_1 + (E_{0m} - E_1)\sin s\omega(t - t_1)$$

and for the third interval ($t_2 < t < \frac{T}{2}$)

$$e_{03} = U_3 = E_1 \frac{e^{\alpha\omega t_1} e^{-\alpha\omega(t - t_2)} - 1}{e^{\alpha\omega t_1} - 1},$$

(8)

where t_1 = the moment of the conclusion of the first (start of the second) interval. (The beginning of the first interval corresponds to t = 0);

t_2 = the moment of conclusion of the second (start of the third) interval;

α = a positive number, the value of which depends upon the steepness of the front of the emf half-wave;

E_1 = the value of the open-circuit emf at the end of the 1st interval;

T = the fundamental period;

$s = \frac{T}{2(t_2 - t_1)}$;

E_{om} = the maximum value of the open-circuit emf.

With appropriate selection of the constants of approximation α, E_1, and t_1, formulas (8) give a sufficiently accurate analytical expression for the open-circuit emf curve within a wide range of values of the generator dimensions which determine the shape of the curve of this emf (length of the air gap, width of the teeth and the tooth division of the rotor). An expression for the second half-wave of the emf may be obtained from the relationship

$e_0(t + \frac{T}{2}) = - e_0(t)$. If the emf curve is given graphically, then the constants of approximation may be obtained with sufficient ease. Here the length of the first interval (t_1) is selected in conformity with the shape of the curve (near the point of inflection). The moment of time $t_2 = \frac{T}{2} - t_1$, since the curve of the emf half-wave is symmetrical with respect to the vertical axis passing through its maximum. The quantity E_1 is determined from the curve (for a given t_1). The constant α may be determined from the formula

$$\alpha = \frac{2}{\omega t_1} \ln \left[1 + \frac{E_1}{E_{\frac{1}{2}}} \right]. \qquad (9)$$

where $E_{\frac{1}{2}}$ is the open-circuit emf for $t = \frac{t_1}{2}$.

In designing generators with narrow rotor teeth, which may be considered as basic [2], the constants of approximation may also be determined approximately from the formulas

$$\left.\begin{aligned} t_1 &\cong \frac{0{,}25}{f}[1 - b_2' + 0{,}5\delta'] \\ \text{and } \alpha &\cong \frac{1}{\pi f t_1} \ln \left[\frac{1}{(1{,}23 + 4{,}54 b_2')\delta'} - 1 \right] \end{aligned}\right\} \qquad (10)$$

where $f = \frac{z_2 n}{60}$, the fundamental frequency of the generator

and z_2 = the number of teeth in the rotor

n = the speed of rotation of the rotor in revolutions per minute

$b_2' = \frac{2b_2}{t_{z_2}}$, the relative width of a rotor tooth (b_2)

$\delta' = \frac{2\delta}{t_{z_2}}$, the relative length of the air gap (δ_2)

t_{z_2} = the tooth division of the rotor at its outer diameter

The ratio $\frac{E_1}{E_{om}} \cong 0.6$-$0.8$ (the average value of 0.7 may be taken in the first approximation).

Depending on the geometry of the toothed zone and the relationship between the dimensions (δ, b_2, and t_{z_2}), the shape of the

open-circuit emf curve may vary within sufficiently wide limits, at times approximating, for example, a rectangular or trapezoidal shape. Sometimes the emf half-wave curve may be approximated by a sinusoidal or other segment. For the conditions mentioned and also for certain others representing combinations of those mentioned, approximating functions may be obtained from expressions (8) by means of simple transformations and in this sense the proposed approximation has sufficient generality. Thus, for example, in the case of a rectangular pulse, its analytic expression may be obtained from formulas (8) by taking $E_1 = E_{om}$ and $\alpha = \infty$. When the half-wave can be approximated by a sinusoidal segment in expressions (8), it is necessary to take $E_1 = 0$, etc.

Substituting expression (8) in equation (7), we obtain, after integration and transformations, an expression for the stator current in the form:

for the first interval $(0 < t < t_1)$

$$i_{s1} = \frac{E_1}{R(e^{\alpha\omega t_1} - 1)}\left[\frac{\rho}{\rho + \alpha\omega} e^{\alpha\omega t} - 1\right] + G_1 e^{-\rho t};$$

for the second $(t_1 < t < t_2)$

$$i_{s2} = \frac{E_1}{R} + \frac{E_{om} - E_1}{z_1}\sin[s\omega(t - t_1) - \varphi_1] + G_2 e^{-\rho(t - t_1)} \qquad (11)$$

for the third $(t_2 < t < \frac{T}{2})$

$$i_{s3} = \frac{E_1}{R(e^{\alpha\omega t_1} - 1)}\left[e^{\alpha\omega t_1}\frac{\rho}{\rho - \alpha\omega} e^{-\alpha\omega(t - t_2)} - 1\right] + G_3 e^{-\rho(t - t_2)},$$

where $z_1 = \sqrt{R^2 + (s\omega L_0)^2}$ and $\varphi_1 = \arctan\frac{s\omega L_0}{R}$.

The time-boundary conditions for the case under consideration have the form:

$$\left.\begin{aligned} i_{g1}(t_1) &= i_{g2}(t_1); \\ i_{g2}(t_2) &= i_{g3}(t_2); \\ i_{g1}(0) &= -i_{g3}\left(\frac{T}{2}\right). \end{aligned}\right\} \qquad (12)$$

Equations (11), together with the time-boundary conditions of (12), lead to a system of three equations, the solution of which enables us to obtain expressions for the constants G_1, G_2, and G_3, thus making it possible to calculate, according to formula (11), the instantaneous value of the stator current at any moment of time within the limits of the half-period. In order to obtain a half-wave of current of opposite polarity, the following relationship may be used

$$i_g(t) = -i_g\left(t+\frac{T}{2}\right). \qquad (13)$$

Expressions (11) may be used to investigate the shape of the current and to calculate its maximum value. They are not convenient for calculating the effective and average values of the current. An approximate calculation of the latter may be made by using not the actual open-circuit emf, but rather a certain equivalent emf (e_e) of rectangular shape, within the limits of the actual half-period as

$$\left.\begin{aligned} e_{e1} &= 0 \text{ when } 0 < t < t_{1e}; \\ e_{e2} &= E_n \text{ when } t_{1e} < t < t_{2e}; \\ e_{e3} &= 0 \text{ when } t_{2e} < t < \frac{T}{2}. \end{aligned}\right\} \qquad (14)$$

and

Expressions for the equivalent current over all the intervals of the half-period may be obtained from the general expressions (11) by taking $E_1 = E_{om} = E_n$, $\alpha = \infty$, $t_1 = t_{1e}$, and $t_2 = t_{2e}$. It is not difficult to show that for the conditions indicated the expressions for the equivalent stator current assume the form:

for the first interval ($0 < t < t_{1e}$)

$$i_{e1} = G_{1e}e^{-\rho t};$$

for the second interval ($t_{1e} < t < t_{2e}$)

$$i_{e2} = \frac{E_n}{R} + G_{2e}e^{-\rho(t-t_{1e})};$$

for the third interval ($t_{2e} < t < \frac{T}{2}$)

$$i_{e3} = G_{3e}e^{-\rho(t-t_{2e})}. \qquad (15)$$

Using the time-boundary conditions (12) for the current (15), we obtain as a result of solving the system of three equations (see above) the expressions for the constants G_{1e}, G_{2e}, and G_{3e} in the form:

$$G_{1e} = -\frac{E_n}{R}e^{-\rho t_{1e}}\left(\frac{1-e^{-\rho t_{ne}}}{1+e^{-\rho\frac{T}{2}}}\right);$$

$$G_{2e} = -\frac{E_n}{R}\left(\frac{1+e^{-2\rho t_{1e}}}{1+e^{-\rho\frac{T}{2}}}\right); \qquad (16)$$

$$G_{3e} = \frac{E_n}{R}\left(\frac{1-e^{-\rho t_{ne}}}{1+e^{-\rho\frac{T}{2}}}\right).$$

where $t_{ne} = t_{2e} - t_{1e}$ is the pulse duration of the equivalent emf.

An expression for the effective value of the equivalent current may be obtained from the formula

$$I_{ee} = \sqrt{\frac{2}{T}\left[\int_0^{t_{1e}} i_{e1}^2 dt + \int_{t_{1e}}^{t_{2e}} i_{e2}^2 dt + \int_{t_{2e}}^{\frac{T}{2}} i_{e3}^2 dt\right]}. \qquad (17)$$

Substituting expressions (15) into formula (17) and taking (16) into account, we obtain, after integration and transformations,

$$I_{se} = \frac{E_n}{R}\sqrt{t_{ne}' - \frac{(1-e^{-\rho_1\pi t_{ne}'})\,[1+e^{-\rho_1\pi(1-t_{ne}')}]}{\rho_1\pi(1+e^{-\rho_1\pi})}}. \qquad (18)$$

where $\rho_1 = \frac{\rho}{\omega}$ and $t_{ne}' = \frac{2t_{ne}}{T}$ is the relative duration of the equivalent emf pulse.

The average value of the equivalent current may be obtained from the formula

$$I_{se\ av} = \frac{2}{I}\left[\int_0^{t_{1e}}(-i_{se1})dt + \int_{t_{1e}}^{t_0}(-i_{se2})dt + \int_{t_0}^{t_{2e}} i_{se2}dt + \int_{t_{2e}}^{\frac{T}{2}} i_{se1}dt\right], \qquad (19)$$

where t_o is the moment of time corresponding to a zero value of the current i_{se2}. For the conditions under consideration the current i_{se} is always negative. The current i_{se2} is also negative over the interval $t_{1e} < t < t_o$, as is easily seen from expressions (15) and (16). Therefore, in the first and second integrals of equality (19) a minus sign is placed before these currents. Substituting expressions (15) into formula (19) and taking (16) into account, we obtain, after integration and transformations

$$I_{se\ av} = \frac{E_n}{R}\left[t_{ne}' - \frac{2}{\rho_1\pi}\ln\frac{1+e^{-\rho_1\pi(1-t_{ne}')}}{1+e^{-\rho_1\pi}}\right]. \qquad (20)$$

the shape factor of the current may be obtained from the ratio

$$K_{\phi i} = \frac{I_{se}}{I_{se\ av}}. \qquad (21)$$

For $0.25 < t_{pe}' < 0.75$ and $\rho_1 > 2.5$, expressions (18) and (20) may be reduced to the simpler approximations:

$$I_{c\phi} \cong \frac{E_n}{R}\sqrt{t_{n\phi}' - \frac{1}{\rho_1 \pi}} \qquad (18a)$$

and

$$I_{c\phi\,av} \cong \frac{E_n t_{n\phi}'}{R}. \qquad (20a)$$

The expression for the shape factor of the current now assumes the form

$$K_{\phi i} \cong \frac{\sqrt{t_{n\phi}' - \frac{1}{\rho_1 \pi}}}{t_{n\phi}'}. \qquad (22)$$

In order that the effective and average values of the equivalent current be as close as possible to the same values of the actual current, let us determine the equivalent emf in such a way that its effective (E_e) and average ($E_{e(av)}$) values will be equal to the corresponding values of the actual open-circuit emf (E_o and $E_{o(av)}$), i.e.,

$$\left.\begin{aligned} E_o &= E_e \\ \text{and } E_{o\,av} &= E_{e\,av}. \end{aligned}\right\} \qquad (23)$$

But the effective and average values of a rectangular pulse of duration t_{pe} are expressed respectively thus:

$$\left.\begin{aligned} E_e &= E_n\sqrt{t_{n\phi}'} \\ \text{and } E_{e\,av} &= E_n t_{n\phi}'. \end{aligned}\right\} \qquad (24)$$

Solving the system of two equations (24) with respect to the unknown maximum value of the equivalent emf E_n and duration t_{ne}', we obtain after simple transformations and with (23) taken into account

$$\left.\begin{aligned} t_{n\phi}' &= \frac{1}{K_{\phi e}^2} \\ \text{and } E_n &= E_{o\,av} K_{\phi e}^2 = E_o K_{\phi e}. \end{aligned}\right\} \qquad (25)$$

where $K_{fe} = \frac{E_o}{E_{o(av)}}$ is the shape factor of the actual emf.

The approximate values of E_o and $E_{o(av)}$ for a SPIG with narrow rotor teeth may be determined from the empirical formulas:

$$\left.\begin{aligned} E_o &\cong E_{om}[(1{,}88 - 5{,}67b_2' + 6{,}67b_2'^2)\delta' + 0{,}21 + 1{,}39b_2' - 0{,}84b_2'^2] \\ \text{and } E_{o(av)} &\cong E_{om}[0{,}031 + 3{,}37\delta' - 15{,}1\delta'^2 + (0{,}99 - 1{,}6\delta')b_2'] \end{aligned}\right\} \quad (26)$$

It should be noted that the errors of the empirical formulas (26) are small and that these formulas may be used for practical calculations over a wide range of change in the dimensions δ' and b_2'. (These formulas were verified over the range of values for $\delta' = 0.01$ to 0.08 and $b_2' = 0.15$ to 0.4, which embraces practically the entire series of possible values of these quantities). Taking equations (22) and (25) into account, we obtain an approximate relationship between the shape factors of the current and the emf in the form:

$$\frac{K_{\Phi i}}{K_{\Phi e}} \cong \sqrt{1 - \frac{K_{\Phi e}}{\rho_1 \pi}} \quad (27)$$

From expression (27) it may be seen that with an increase in the load current the shape factor of the current decreases; moreover, the stronger the load current for the same ρ_1, the greater the shape factor of the emf, i.e., in other words, the sharper the emf curve. If it is assumed during loading that the shape factor of the current cannot decrease by more than 10% in comparison with the shape factor of the emf, then, for $K_{\Phi e} = 1.5$, which may be considered as close to the minimum permissible in the case of electroerosion processing, we obtain from formula (27) the value $\rho_1 \geqslant 3$.

Given a steady excitation current, the voltage at the terminals of the generator decreases with an increase in the load current. The decrease in voltage may be characterized by the ratio

$$\Delta U = \frac{E_o - U_{cl}}{E_o}, \quad (28)$$

where E_o is the open-circuit voltage and U_{se} is the voltage under load. The effective value of the voltage $U_{se} = R_1 I_{se}$, whence, taking into account Eqs. (18a), (25) and (28) and also the fact that usually $R_1 \sim R$, we obtain after transformations

$$\Delta U \quad 1 - \sqrt{1 - \frac{K_{\phi e}^2}{\rho_1 \pi}} \tag{29}$$

or taking Eq. (27) into account

$$\Delta U - 1 - \frac{K_{\phi i}}{K_{\phi e}}. \tag{30}$$

From Eq. (29) it may be seen that the decrease in voltage, all other conditions being equal, is all the greater, the greater the shape factor of the open-circuit emf. In other words, the effective value of the voltage is all the less, all other conditions being equal, the sharper the open-circuit emf curve (or the lower its pulse duty factor). From Eq. (30) it may be seen that a reduction in voltage depends on the degree of distortion of the shape of the current curve with respect to the emf curve.

By means of similar transformations, using Eq. 20, it is possible to obtain a formula for the decrease in the average voltage in the form

$$\Delta U_{av} = \frac{E_{o\,av} - U_{e\,av}}{E_{o\,av}} = \frac{2K_{\phi e}^2}{\rho_1 \pi} \ln \frac{1 \quad e^{-\rho_1 \pi (1 - t_{n\Phi}')}}{1 + e^{-\rho_1 \pi}}, \tag{31}$$

from which it is apparent that the decrease in the average value of the voltage, all other conditions being equal, is all the greater, the sharper the open-circuit emf curve. It may also be seen from Eq. (31) that the decrease in the average value of the voltage is relatively small.

In calculating the external characteristics relating the effective values of the stator current and the stator terminal voltage

(assuming that i_{fo} = const and n = const), the solution of differential equation (6) is more conveniently represented in the form of a Fourier series. A series expansion of the open-circuit emf may be accomplished with the aid of well-known graph-analysis methods; however, the coefficients of the series can be determined more simply and accurately enough analytically by using expressions (8).

In the system of coordinates used in approximating (8) the open-circuit emf is an odd function of time, and, consequently, its Fourier series should contain only sinusoidal terms. Moreover, since the condition $e_o(t + \frac{T}{2}) = -e_o(t)$ is always satisfied in the case of the emf of symmetrical pulse generators, this series contains only odd harmonics, i.e.,

$$e_0(t) = \sum_{k=1,3,5,\ldots} E_{om} E_{ok}' \sin k\omega t, \qquad (32)$$

where $E_{ok}' = \frac{E_{ok}}{E_{om}}$ is the relative amplitude of the k-th harmonic of the open-circuit emf (the introduction of relative amplitudes may be convenient in making conversions).

The values of the relative amplitudes may be found from the well-known formula

$$E_{ok}' = \frac{4}{T}\int_0^{\frac{T}{2}} e_o'(t) \sin k\omega t \, dt, \qquad (33)$$

where $e_o' = \frac{e_o(t)}{E_{om}}$ is the relative instantaneous value of the open-circuit emf. Substituting expressions (8) into formula (33), we obtain, after integration and well-known transformations

$$E_{ok}' = \frac{4}{\pi}\left\{\frac{E_1'}{e^{\pi\alpha t_1'} - 1}\left[\frac{e^{\pi\alpha t_1'}(\alpha \sin k\pi t_1' - k\cos k\pi t_1') + k}{k^2 + \alpha^2} - \right.\right.$$
$$\left.\left. - \frac{1 - \cos k\pi t_1'}{k}\right] + \frac{E_1'}{k}\cos k\pi t_1' + \frac{(1 - E_1')}{s^2 - k^2} \sin k\pi t_1' \right\}, \qquad (34)$$

where $E_1' = \frac{E_1}{E_{om}}$; $t_1' = \frac{2t_1}{T}$ and $s = \frac{1}{1 - 2t_1'}$.

In the calculations we can usually take into account the first three or four harmonics and neglect the others. After determining the values of the amplitudes of the emf harmonics, we can then calculate, according to well-known formulas, the effective values of the current harmonics and the voltage at the terminals of the stator, respectively, as:

$$\left.\begin{aligned} I_{s\kappa} &= \frac{E_{o\kappa}'}{\sqrt{2}} \frac{E_{om}}{z_\kappa} \\ \text{and } U_{s\kappa} &= I_{s\kappa} z_{\kappa 1}. \end{aligned}\right\} \qquad (35)$$

where z_k and z_{k1} are the total resistances of the stator and load circuits, respectively, for the k-th current harmonic. The effective values of the stator current and the voltage at its terminals are determined according to the formulas:

$$\left.\begin{aligned} I_s &= \sqrt{\sum_k I_{s\kappa}^2} \\ \text{and } U_s &= \sqrt{\sum_k (I_{s\kappa} z_{\kappa 1})^2}. \end{aligned}\right\} \qquad (36)$$

After calculating, according to the above formulas, a series of values of the current and voltage for fixed values of the load parameters, which are varied according to a definite law, it is then possible to plot the external characteristic from the points.

Similarly, other statistical characteristics may also be calculated. It is first necessary to determine the shape and magnitude of the open-circuit emf for a given excitation current. It must be kept in mind that, depending on the magnitude of the excitation current, not only the maximum value, but also the shape of the emf curve varies as a result of a variation in the saturation of the magnetic circuit, the main influence on the maximum value of the

open-circuit emf being the saturation of the casings of the stator and the rotor (and the shields in the single-package design), whereas the main influence on the emf shape is the saturation of the toothed zone and, in particular, the saturation of the rotor teeth. Reduction of the emf amplitude as a result of saturation of the casings of the stator and the rotor (and the shields) may be evaluated by the usual methods when calculating the magnetic circuit. The variation in the shape of the emf as a consequence of saturation of the teeth may be evaluated approximately by assuming that it has the same effect as an increase in the length of the air gap. Consequently, when calculating the emf curve with saturation taken into account, it is necessary to use the value of the equivalent air gap (δ_e)

$$\delta_e = \delta\left(1 + \frac{F_{z1} + F_{z2}}{F_\delta}\right), \qquad (37)$$

where δ is the length of the actual air gap and F_{z1}, F_{z2}, and F_δ are the magnetic stresses of the teeth of the stator, rotor, and air gap, respectively.

The assumptions underlying the theoretical investigation, as well as the basic differential equation (6) and certain other results obtained from a theoretical consideration, were verified experimentally on a number of machines. Given below are certain results of an experimental investigation of a test model of a SPIG with narrow rotor teeth and of two-package design (nominal frequency of alternating emf being 1,000 cps at a rotational speed n of 2,400 rpm; the effective value of the nominal stator current I_s equal to 20 amps), as well as a comparison of the calculated and experimental data.

The inductance of the stator winding was determined experimentally with a stationary rotor. For this purpose, the stator winding was fed a sinusoidal current, and both the voltage drop across it and the

current were measured. According to differential equation (6), the average value of the inductance should be used. Therefore, the limiting values of the inductance, corresponding to two positions of the rotor, were first determined experimentally. The maximum value (L_{max}) corresponds to the position at which the axis of the coil of the stator winding coincides with the axis of the rotor tooth, while the minimum value (L_{min}) corresponds to the position at which the axis of the coil of the stator winding coincides with the axis of the rotor groove. The average value of the inductance was obtained from the formula

$$L_o = \frac{L_{max} + L_{min}}{2}. \qquad (38)$$

For the machine described, the limiting and average values of the inductance, determined at a stator current frequency of 50 cps, were equal to

$$L_{max} = 6.13 \cdot 10^{-4} \text{ h}; \quad L_{min} = 5.01 \cdot 10^{-4} \text{ h}$$
$$\text{and } L_o = 5.57 \cdot 10^{-4} \text{ h}$$

Note that the average value of the inductance determined at a frequency of 500 cps was practically the same as at 50 cps.

In order to check differential equation (6a) and certain formulas obtained from a theoretical consideration, a comparison of the calculated and experimental data is presented below. Figure 2 shows the curve of the open-circuit emf half-wave obtained experimentally from an oscillogram (solid line), recorded at an excitation current $i_{ex} = 0.8$ amp. In the same figure the graph of the emf half-wave obtained by calculating according to formula (8) is shown as a broken line. In this case the following values were taken for the

approximation constants: $\alpha = 3$; $\frac{E_1}{E_{om}} = 0.7$; $t_1' + 0.36$ and $t_2' = 1 - t_1' = 0.64$. (Determined from the experimental curve presented in Fig. 2).

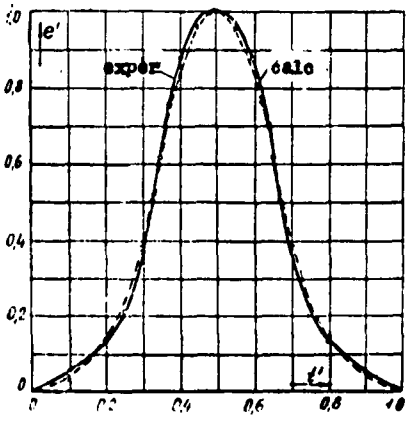

Fig. 2. Electromotive force of a SPIG ($i_{ex} = 0.8$ amp.; f = 1,000 cps).

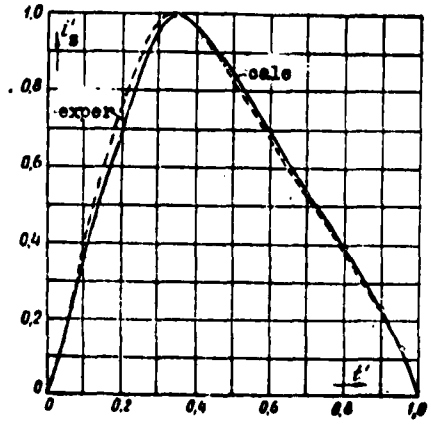

Fig. 3. Stator current of a SPIG ($R = 2.7$ ohms, $L_o = 5.57 \cdot 10^{-4}$ h; f = 1,000 cps).

Both graphs were constructed in relative units, where the relative value of the time t was determined as $\frac{2t}{T}$, while the relative values of the instantaneous emf's $e_o(t)$ were determined as $\frac{e_o(t)}{E_{om}}$. It can be seen from the figure that the calculated graph agrees very closely with the experimental graph. A quantitative comparison indicates that the greatest relative deviation of the ordinates of the experimental and calculated curves does not exceed 0.03. The ratio between the average values of the calculated and experimental emf is $\frac{E_{oav(calc}}{E_{oav(exper)}} = 0.995$, while the ratio between their effective values is $\frac{E_{o(calc)}}{E_{o(exper)}} = 0.99$. (The average and effective

values of both emf's were determined by the same method of graph analysis). The shape factors for the calculated and experimental curves are 1.39 and 1.396, respectively.

The above comparison indicates a sufficiently close agreement between the calculated and experimental emf's. Figure 3 shows current curves, one of which was obtained experimentally (from an oscillogram) and is indicated by a solid line, while the other, indicated by a broken line, was obtained by calculation from formula (11) with the above-given values of the approximation constants. The above-given value of the inductance was used in the calculation. Both curves were plotted in relative units with the basis of the relative magnitudes of the current being the maximum value of the current, as determined from the graph.

The magnitude of the active resistance of the stator winding was determined approximately in the assumption that it exceeds the magnitude of the ohmic resistance by 20%. The active resistance thus determined amounted to $r_s = 0.15$ ohms. The measured ohmic resistance of the load, R_1 amounted to 2.5 ohms. It should be noted that the load rheostat used in the experiments was made of thin manganin tape applied bifilarly. Therefore its inductance was not taken into consideration in the calculations. Moreover, the skin effect in such a rheostat is obviously insignificant, and therefore it was assumed that its ohmic resistance was equal to its active resistance. The total resistance of the stator circuit was taken to be $R = 2.7$ ohms.

The maximum value of the open-circuit emf, measured before loading, was found to be $E_{om} = 290$ volts. The experimental emf frequency was $f = 1{,}000$ cps.

It is apparent from Fig. 3. that the calculated curve is in

sufficiently close agreement with the experimental curve. The greatest difference between the relative magnitudes (instantaneous) of current amounts to about 0.05. The ratio between the average values of the current (calculated to experimental) is $\frac{I_{sav(calc)}}{I_{sav(exper)}} =$ $= 1.005$, while the ratio between the effective values is $\frac{I_{s(calc}}{I_{s(exper)}} = 1.008$. The shape factors of the calculated and experimental curves are 1.15 and 1.149, respectively. A satisfactory agreement between the calculation and the experiment is also obtained for the absolute values of the current. In accordance with differential equation (6a), the maximum value of the current may be determined as

$$I_{sm} = \frac{e_o(t_m)}{R}, \qquad (39)$$

where t_m is the moment of time corresponding to the maximum current and $e_o(t_m)$ is the open-circuit value of the emf at the moment of time $t = t_m$. The relative value of the time t_m, determined from the graphs, amounted to 0.68, while the value $e_o(t_m)$ determined from formula (8) for the third interval, was found to be $e_o(t_m) = U_3(t_m) =$ $= 137$ volts. The maximum value of the current, determined from formula (39), was $I_{sm(calc)} = 50.7$ amp. The maximum measured value of the current was $I_{sm(exper)} = 49.5$ amp., i.e., with respect to the experimental value, the error in the calculation amounts to only about 2.5%.

Figure 4 shows the external characteristic (solid line), calculated from formulas (34) - (36), for a purely active generator load with an excitation current $i_{ex} = 1$ amp and a frequency $f = 1000$ cps. In the calculation of this characteristic the circuit parameters,

L_0 and r_s, obtained experimentally (see above), and also the measured effective value of the open-circuit emf E_0 = 172.6 volts, were used.

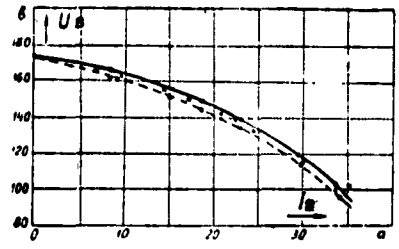

Fig. 4. External characteristic of a SPIG (i_{ex} = 1.0 amp; f = 1,000 cps; $z_1 = R_1$). ————calculation according to formulas (34) - (36); – – – – – – calculation according to formula (18); x x x x x experiment (i_{ex} = 1.0 amp; f = 1,000 cps).

Since, as is hown by experiment, the saturation of the magnetic circuit by a current i_{ex} = 1 amp is relatively small, the values of the approximation constants were taken to be the same as for a current i_{ex} = 0.8 amp (see above).

Only the first three harmonics of the open-circuit emf were taken into account in the calculation. The maximum value of the open-circuit emf, which is necessary for the calculation, was determined from the ratio $E_m = \frac{E_0}{E_0'}$, while the relative effective value with formula (34) taken into account was taken as

$$E_0' \cong \sqrt{\frac{E_{01}'^2 + E_{03}'^2 + E_{05}'^2}{2}} =$$

$$= \sqrt{\frac{0{,}683^2 + (-0{,}283)^2 + 0{,}05^2}{2}} = 0{,}524.$$

Figure 4 also shows the points of the external characteristic which were determined by experiment. It can be seen that the calculated data agree satisfactorily with the experimental data. The broken line on this same figure shows the external characteristic calculated by means of approximation formula (18). The data from the approximate calculation also agree satisfactorily with the experimental data, thus corroborating the admissibility of using formula (18) for approximate calculations.

The current shape factor, calculated from approximation formulas (18) and (20), corresponds to the current in Fig. 3 and has a value of 1.11.

The experimental results and also the comparison between the experimental data and the calculations thus corroborate the admissibility of the assumptions made in deriving equation (6), as well as the accuracy of the basic calculation equations obtained. It should be noted that the derived differential equation (6) applies in full measure to ordinary inductance generators of like-pole design.

REFERENCES

1. A. L. Livshits and I. S. Rogachev. High-Current Periodic-Pulse Generators, GEI (State Power Engineering Institute), 1959.

2. I. S. Rogachev and A. N. Tkachenko. Unipolar-Pulse Induction Generators with External Rectifiers, "Elektromekhanika", 1960, No. 4.

3. V. F. Tabachinskiy. Graph-Analysis Method of Determining the Current in a Circuit Connected to a Nonsinusoidal Voltage. "Elektrichestvo", No. 11, 1953.

4. S. I. Kurenev. The Calculation of Circuits in the Presence of Periodically Interrupted or Pulse Voltages, "Elektrichestvo", No. 12, 1953.

5. I. S. Gonorovskiy. Radio Signals and Transient Phenomena in Radio Circuits, State Publishing House of Literature on Problems of Communication and Radio, 1954.

6. I. S. Rogachev. The Shape of the Curve of the Field Distribution in Machine Pulse Generators. Proceedings of the V. I. Lenin Polytechnic Institute in Kharkov, Vol. XX, No. 1, 1958, Electrical-Machine Construction Series.

Submitted on March 8, 1961.

A MATHEMATICAL ANALOG OF TRANSIENTS OF A SYNCHRONOUS MACHINE USING EXPERIMENTAL DYNAMIC CHARACTERISTICS

Yu. A. Bakhvalov

As is known, the analytic study of transient regimes of electrical machines is made difficult by the fact that the equations describing these regimes are nonlinear, even when saturation of the steel parts of the machine is not taken into account. Therefore, in analysis of the operation of electrical machines, for example, in the study of static and dynamic stability, electronic computers must find wide application [1, 2, 3, 4, 9].

The applied sciences are constantly striving toward a more accurate expression of physical phenomena, by taking into account all existing factors. This has been especially intensified recently, due to the advent of electronic computers.

However, the practical realization of this meets with obstacles. Firstly, the absence of prepared algorithms for the solution of problems, and, secondly, the insufficient capability of computers (for analog machines, the limited number of solving units and the lack of a "memory").

These obstacles can sometimes be overcome by the use of experimental dynamic characteristics. It should be noted that the use of experimental dynamic characteristics has shown its advantageousness even in cases not connected with computer technology. For example, in the analysis of transients in a-c electrical machines, by the suggestion of Kazovskiy [5], frequency characteristics are used, which allow a sufficiently complete description of the dynamic properties of electrical machines to be made, since there the electrical contours of the rotor are taken into account, which are determined by the presence in it of massive parts.

Thus it must be acknowledged that the characteristic of electrical machines with static parameters used at the present time is incomplete, and factories must also give dynamic characteristics in the catalogs of their machines.

The present article shows the use of experimental dynamic characteristics of synchronous machines in solving a nonlinear problem by an analog. As will be seen later on, the use of experimental characteristics for an analog on a continuous-action electronic computer allows the number of solving units to be reduced considerably, preserving the essential properties of the object to be simulated.

The essence of the proposed method is as follows. In the object under study, elements are isolated whose properties were obtained as experimental dynamic characteristics. These characteristics allow, by the use of a Laplace-Carson operator transform, the parameters of electrical circuits having similar characteristics to be obtained comparatively simply. The electrical processes in these circuits are simulated by using continuous-action electronic computers. Since methods of determining operator functions by experimental dynamic

characteristics has been covered in detail in the literature [6, 7], main attention is now devoted to the problem of synthesis of electrical circuits by given operator functions, and to the use of the circuits obtained for constructing an analog of the object under study.

In the present work, a synchronous machine is examined from the point of view of circuit theory. This means that it can be represented by a system of magnetically coupled coils with steel cores. Therefore, when making an analog of a synchronous machine, let us use the method of simulation of a coil with a steel core for a given transient response (Appendix 1).

1. An Analog of a Synchronous Salient-Pole Machine Without Taking Saturation into Account

Let us examine the symmetric regimes of a machine which operates in parallel with a system of infinite power without a zero wire. The upper harmonics of the magnetic field of the machine are not taken into account. Let us use the system of equations of the synchronous machine transformed to the axes d and q. This system is the most convenient for an analog, since it does not contain periodic coefficients. Let us assume that along each axis all contours are covered by the total flux of mutual inductance. In addition, each contour has its own leakage flux. The initial regime is the motor regime. All values are expressed in relative units. Let the base current of the rotor be the current of the field coil, which compensates for the reaction of the starting winding, which conducts a nominal current in the short-circuit regime. First of all, let us examine the analog of a synchronous machine whose magnetic system is unsaturated.

The stator equations:

$$u_d = i_d r + \frac{d\psi_d}{dt} - \omega\psi_q, \tag{1}$$

$$u_q = i_q r + \frac{d\psi_q}{dt} + \omega\psi_d, \tag{2}$$

$$\psi_d = i_d x_d + (i_v + i_{d1} + \ldots + i_{dn}) x_{ad}, \tag{1a}$$

$$\psi_q = i_q x_q + (i_{q1} + \ldots + i_{qn}) x_{aq}, \tag{2a}$$

$$\left.\begin{aligned} u_d &= -U_m \sin\delta, \quad u_q = U_m \cos\delta, \\ \omega &= 1 - \frac{d\delta}{dt}. \end{aligned}\right\} \tag{3}$$

The equations of the field coil:

$$u_v = i_v r_v + \frac{d\psi_v}{dt}, \tag{4}$$

$$\psi_v = i_v x_v + (i_d + i_{d1} + \ldots + i_{dn}) x_{ad}. \tag{4a}$$

The equations of the additional rotor contours (artificial damping contours and natural contours which depend upon the presence of massive parts whose number is not established beforehand):

along the d axis

$$0 = i_{dj} r_{dj} + \frac{d\psi_{dj}}{dt}, \tag{5}$$

$$\psi_{dj} = i_{dj} x_{dj} + (i_d + i_v + i_{d1} + \ldots + i_{dj-1} + i_{dj+1} + \ldots + i_{dn}) x_{ad}, \tag{5a}$$

$$j = 1, 2, \ldots, n.$$

along the q axis

$$0 = i_{qj} r_{qj} + \frac{d\psi_{qj}}{dt}, \tag{6}$$

$$\psi_{qj} = i_{qj} x_{qj} + (i_q + i_{q1} + \ldots + i_{qj-1} + i_{qj+1} + \ldots + i_{qm}) x_{aq}, \tag{6a}$$

$$j = 1, 2, \ldots, m.$$

The equation of motion

$$T_a \frac{d^2\delta}{dt^2} = m_a - (\psi_d i_q - \psi_q i_d). \tag{7}$$

It is difficult to make an analog of system of equations (1) through (7), because calculation of the parameters of the additional contours is very complicated. Consequently, let us use experimental dynamic characteristics.

Having transformed linear Eqs. (1a), (2a), (4), (4a), (5), (5a), (6), and (6a) into operator form and excluded the currents of the rotor

circuits, we obtain the following system of operator equations:

$$\Psi_d(p) = G(p)U_v(p) + x_d(p)I_d(p), \tag{8}$$

$$\Psi_q(p) \quad x_q(p)I_q(p). \tag{9}$$

Now the transients of the synchronous machine are described by Eqs. (1), (2), (3), (7), (8) and (9).

Equations (8) and (9) contain unknown operator coefficients $x_d(p)$, $x_q(p)$, $G(p)$, which are determined by the parameters of the contours of the machine. Let us establish which characteristics must be taken at the object of study in order to determine these coefficients.

The functions $x_d(p)$ and $x_q(p)$ can be obtained most simply if we let $U_v(p) = 0$ and $\omega = 0$. Then Eqs. (1) and (2), which become linear at $\omega = 0$, after transformation to operator form and substitution of Eqs. (8) and (9) (at $U_v(p) = 0$), take the form

$$\left.\begin{aligned} U_d(p) &= I_d(p)[r + px_d(p)] = I_d(p)Z_d(p), \\ U_q(p) &= I_q(p)[r + px_q(p)] = I_q(p)Z_q(p). \end{aligned}\right\} \tag{10}$$

From (10) and the conditions $U_v(p) = 0$ and $\omega = 0$ it is apparent that the expressions $Z_d(p)$ and $Z_q(p)$ are the operator impedances along the d and q axes of the stator windings of a fixed synchronous machine with short-circuited field coil.

Solving Eqs. (10) for the currents at $U_d(p) = U_q(p) = 1$, we obtain

$$\left.\begin{aligned} I_d(p) &= \frac{1}{Z_d(p)} = Y_d(p) \doteq i_d(t), \\ I_q(p) &= \frac{1}{Z_q(p)} = Y_q(p) \doteq i_q(t). \end{aligned}\right\} \tag{11}$$

In order to obtain the transient response $i_d(t)$ experimentally, the rotor must be placed in a position in which the rotor axis d coincides with the magnetic axis of the stator winding. To obtain $i_q(t)$, the d axis must be perpendicular to the magnetic axis of the

stator winding.

The stator winding is fed from a d-c source. The field coil is short circuited or has a working resistance across it. The rotor is fixed. The magnetic system is unsaturated.

By making oscillographs of currents $i_d(t)$ and $i_q(t)$ after shunting the stator winding ($t = 0$), and reducing the obtained transient responses to $u_d = u_q = 1$, on the basis of (11) we will have data for constructing the functions $Y_d(p)$ and $Y_q(p)$ (Appendices 1 and 3), and, therefore, $x_d(p)$ and $x_q(p)$. A detailed description of experiments for taking the curves of $i_d(t)$ and $i_q(t)$ has been given [11, 5].

To determine $G(p)$ by using Eq. (8), it is necessary to obtain the function $\Psi_d(p) \rightarrow \psi_d(t)$ at $I_d(p) = 0$. The transient response $\psi_d(t)$ can be found by the following experiment. The machine is disconnected from the power ($i_d = i_q = 0$) and turns with a synchronous speed ($\omega = 1$). The field coil at time $t = 0$ is connected to a d-c source u_v. The emf of phase a of the stator is determined by the relation

$$e_a = e_d \cos \omega t + e_q \sin \omega t.$$

Using Eqs. (1) and (2) at $i_d = i_q = 0$ and $\omega = 1$, we have

$$e_d = -\frac{d\psi_d}{dt}, \quad e_q = -\psi_d.$$

The magnitude of $\frac{d\psi_d}{dt}$ in our experiment is less than one per cent of ψ_d, since the time constant of the field coil is high. Therefore, it can be assumed that

$$e_a \cong -\psi_d \sin \omega t.$$

Thus the envelope of the curve of $e_a(t)$ gives the function $\psi_d(t)$. In order to eliminate the effect of the source u_v, the experiment is better performed with shunting at time $t = 0$ of the field coil, which

is fed from source u_v. Reducing the curve obtained $\psi_d(t)$ to $u_v(-0) = 1$ and using the Laplace-Carson transform, we obtain $\Psi_d(p) = G(p)$ (Appendices 1 and 3).

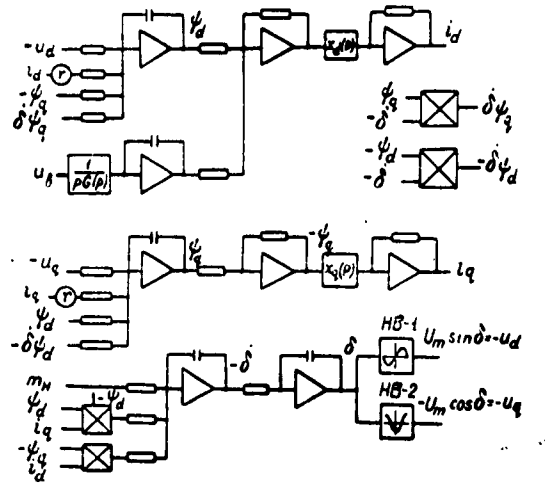

Fig. 1. Diagram of analog of synchronous machine constructed from parameters obtained from transient responses.

From functions $x_d(p)$, $x_q(p)$ and $G(p)$ obtained, let us construct equivalent circuits which realize these functions. Then, in accordance with Eqs. (1), (2), (3), (7), (8) and (9), let us set up the circuit of the analog of the synchronous machine (Fig. 1). The circuit obtained contains 9 computer amplifiers, independent of the number of additional rotor contours, while the analog circuit for system of equations (1) through (7) at $n = m = 1$ will contain 17 amplifiers; at $n = m = 2$ there will be 23 amplifiers.

The analog of an actual synchronous motor by circuit (Fig. 1) showed good agreement between results of the calculation with the analog of the experiment (Appendix 3).

2. An Analog Taking Saturation into Account

This method makes it possible to take saturation of the steel into account by introducing certain complexities into the circuit.

Let us examine the construction of the analog of a synchronous machine taking saturation of the steel into account only along the d axis. Let us assume that the leakage fluxes are linear functions of the currents in the contours, and only the inductive reactance of the mutual inductance x_{ad} is a function of the regime. In this case saturation is easily taken into account in those cases when x_{ad} is isolated by a separate branch. To construct an analog taking saturation into account on a fixed unsaturated machine, oscillographs are made of the curves of $i_d(t)$ and $i_q(t)$, and also the curve of current loss in the field coil $i_v(t)$ when it is shunted at time $t = 0$. At $t < 0$ the field coil is fed from a d-c source. In addition, the characteristic of the no-load condition of the machine is taken; the emf of the stator in the function of the excitation current $e = f(i_v)$, which, in relative units, represents the function $\psi_{ad} = f(i_v)$ (since $e = \psi_{ad}$, where ψ_{ad} is the inter-linkage of the mutual inductance).

If the inductive reactance of the stator winding x_σ is known from an additional experiment [11]), then, by using the transient responses $i_d(t)$ and $i_q(t)$, we can construct equivalent circuits of the machine for the d and q axes, the structure of which is chosen from physical considerations (Appendix 1). In these circuits, reactances x_{ad} and x_{aq} (unsaturated values) are isolated in separate branches.

Let us represent the saturated value $x_{ad}^H = \varphi(\psi_{ad})$ in the form

$$x_{ad}^H = s \cdot x_{ad},$$

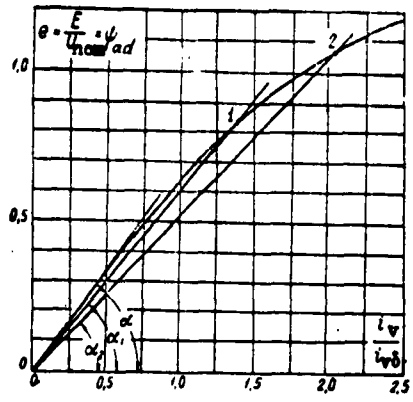

Fig. 2. Characteristic of no-load conditions of 7-kva synchronous machine (base current of rotor $i_{v\delta}$ = 1.1 a)

where s is a function of the interlinkage ψ_{ad}. For the unsaturated part of the characteristic $\psi_{ad} = f(i_v)$, s = 1. The value of s in the saturated part is found by the relations

$$s_1 = \frac{\tan \alpha_1}{\tan \alpha}, \quad s_2 = \frac{\tan \alpha_2}{\tan \alpha}$$

etc. (Fig. 2).

Having transformed Eqs. (1a), (4a), (5) and (5a) into operator form and excluded the currents of the additional contours, we obtain the following equations:

$$\Psi_d(p) = I_d(p)x_d + \Psi_{ad}(p), \tag{12}$$

$$\Psi_v(p) = I_v(p)x_{v\sigma} + \Psi_{ad}(p), \tag{13}$$

$$\Psi_{ad}(p) = [I_d(p) + I_v(p)]x_{ad}'(p), \tag{14}$$

where $x_{v\sigma}$ is the inductive reactance of the leakage of the field coil; and $x_{ad}'(p)$ the inductive operator reactance of mutual inductance along the d axis when the field coil is open.

Transient response $i_d(t)$ is taken when the field coil is closed, which makes it possible to determine the equivalent parameters of the additional contours under conditions of actual distribution of the magnetic field in the rotor. Therefore, we obtain a circuit for $x_{ad}'(p)$ from the circuit of $x_d(p)$, constructed using the curve of $i_d(t)$, by discarding the element $R \equiv x_\sigma$ and disconnecting the circuit corresponding to the field coil. In order to determine this current it is necessary to know the time constant of the field coil. The latter can be found by using the curve of $i_v(t)$. For this, $Z_v(p)$ is found on the curve of $i_v(t)$ (Appendix 1). Then the time constant

$$T_v = \frac{[X_v(p)]_{p=0}}{R_v} = \frac{\left\{\frac{1}{p}[Z_v(p) - R_v]\right\}_{p=0}}{R_v}.$$

The value of T_v allows the parameters of the field coil x_v and r_v, reduced to the stator winding, to be established from the circuit obtained for $x_d(p)$.

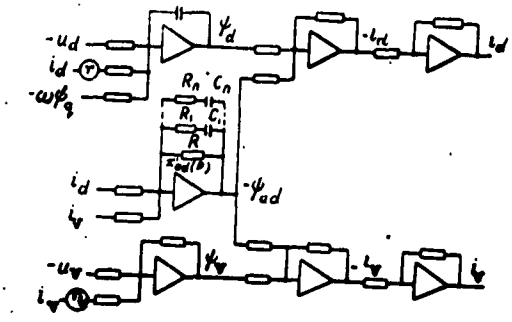

Fig. 3. Circuit of analog of synchronous machine along d axis: $R \equiv x_{ad}$, $R_1 \equiv x_{d1}$, ..., $R_n \equiv x_{dn}$, $C_1 \equiv \frac{1}{r_{dn}}$ are determined by the method given in Appendix 1.

One possible circuit of an analog of a synchronous machine for the d axis, set up using Eqs. (1), (3), (4), (12), (13) and (14), is shown in Fig. 3.

Circuits of an analog for the q axis and the equations of motion remain as before (Fig. 1).

The function $x_{ad}^H = \varphi(\varphi_{ad})$ in the analog can be realized in various ways.

The first method is by using a nonlinear unit. In this we shall vary not the parameter x_{ad} itself, but the voltage u supplied to $R \equiv x_{ad}$. This voltage will be assumed a function of ψ_{ad} of the form $u \equiv s^{-1}\psi_{ad}$, where s^{-1} is a function, the reciprocal of s, set up in the nonlinear unit. The latter is connected in series with $R \equiv x_{ad}$

(Fig. 4a). In regimes corresponding to saturation of the steel, the voltage u and the current through $R \equiv x_{ad}$ will increase, which is equivalent to a decrease in x_{ad}^{H}.

The second method is by using a programmed control circuit. In this case the function $x_{ad}^{H} = \varphi(\psi_{ad})$ is approximated by a step curve. In accordance with this curve, x_{ad} is varied stepwise by using a programmed control circuit, which is a set of amplifiers. A relay is connected to the output of these amplifiers. The relay contacts are connected in parallel with $R \equiv x_{ad}$ new resistances. The relay operates when $u \equiv \psi_{ad}$ reaches certain values.

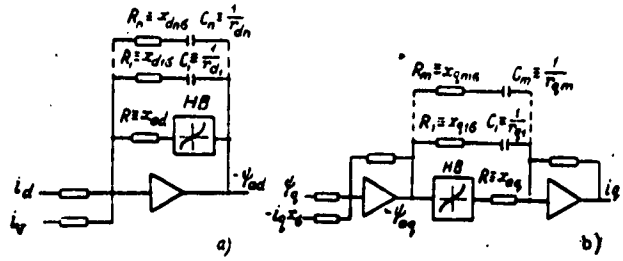

Fig. 4. Taking saturation of steel into account in the analog.

The saturation along the q axis is taken into account similarly; complication of the circuit of the analog consists of adding a nonlinear unit and one solving amplifier (Fig. 4b), or a programmed control circuit.

Use of the second method allows the effect upon saturation along one axis of fluxes along the other axis to be taken into account. It can be assumed approximately that inductive reactances x_{ad} and x_{aq} are functions of the absolute value of the total interlinkage of the armature reaction

$$|\psi_a| = \sqrt{\psi_{ad}^2 + \psi_{aq}^2}.$$

The value $|\psi_a|$ can be obtained on a separate circuit and fed to the programmed control circuit.

Conclusions

1. An analog of synchronous machines based on experimental dynamic characteristics can be made with comparatively few computers.

2. An analog of a synchronous machine based on Park-Gorev equations with the use of experimental dynamic characteristics gives results which agree with experiments with a sufficient degree of accuracy.

3. In addition to the static parameters, it is necessary to include dynamic characteristics in the catalogs of synchronous machines.

Appendix 1

An Analog of a Coil with an Unsaturated Steel Core

Let us make the following assumptions: 1) the core is unsaturated; 2) the action of the eddy currents is equivalent to the action of a system of contours (the number of contours is not established beforehand); and 3) all contours are covered by a single total flux passing through the steel. In addition, each contour has a leakage flux which is connected only with that contour.

On the basis of these assumptions, the processes in a coil with a core are described by the following system of equations:

$$\left.\begin{aligned} u_1 &= i_1 r_1 + L_{1\sigma}\frac{di_1}{dt} + \frac{d\psi_0}{dt},\\ 0 &= i_2' r_2' + L_{2\sigma}'\frac{di_2'}{dt} + \frac{d\psi_0}{dt},\\ &\cdots\cdots\cdots\cdots\\ 0 &= i_n' r_n' + L_{n\sigma}'\frac{di_n'}{dt} + \frac{d\psi_0}{dt},\\ \psi_0 &= M(i_1 + i_2' + \ldots + i_n'),\\ M &= L_{11} - L_{1\sigma}. \end{aligned}\right\} \qquad (15)$$

where

u_1, i_1 are the voltage and current of the coil;

i_2', ..., i_n' the currents of the secondary contours, reduced to the number of turns of the coil;

L_{11}, r_1 the total inductance and resistance of the coil;

$L_{1\sigma}$ the leakage inductance of the coil;

$L_{2\sigma}'$, ..., $L_{n\sigma}$, r_2', ..., r_n' the leakage inductances and resistances of the secondary contours, reduced to the number of turns of the coil.

Transforming system (15) into operator form and excluding the currents of the secondary contours, we obtain an equation of a coil with a core, which is replaced by a system of contours in the following form:

$$U_1(p)=I_1(p)r_1+L_{1\sigma}pI_1(p)+pL(p)I_1(p)= \\ =I_1(p)Z_{11}(p), \tag{16}$$

where

$$Z_{11}(p)=r_1+pL_{1\sigma}+pL(p)=r_1+pL_{11}(p). \tag{17}$$

From Eq. (16) it follows that

$$I_1(p)=\frac{U_1(p)}{Z_{11}(p)}=U_1(p)Y_{11}(p)\div i_1(t). \tag{18}$$

Here L(p) is a rational operator function whose coefficients are expressed in terms of the parameters. Since the parameters of the secondary contours are very difficult to calculate, a coil with a core will be characterized by an experimental transient response.

The transient response is found as follows. A d-c voltage with a magnitude such that the core is unsaturated is passed through the coil. Then the coil is short-circuited and an oscillograph of the current in it $i_1(t)$ is made. The curve of $i_1(t)$, as is apparent from relation (18), contains information about all contours. Transition from $i_1(t)$ to the transient conductivity, and then to the Laplace-Carson transform gives the function $Y_{11}(p)$. The value of $Y_{11}(p)$

makes it possible to determine $i_1(t)$ analytically for various laws of application of the voltage $u_1(t)$. If a circuit with a given conductivity is constructed, then, by supplying a voltage $u_1(t)$ varying by any law to this circuit, we can observe the curve of $i_1(t)$ on an oscilloscope screen. This circuit will be an analog of a coil with core.

Let us examine the construction of this analog.

Assuming that the curve of $i_1(t)$ is obtained at $u_1(-0) = 1$ and $u_1(0) = 0$, let us break it down into a sum of exponential curves (Appendix 2).

After this we find the transient conductivity

$$y_{11}(t)=C_0-\sum_{i=1}^{n} C_i e^{p_i t}. \tag{19}$$

where

$$C_0=\sum_{i=1}^{n} C_i=\frac{1}{r_1},$$

since $y_{11}(0) = 0$.

Using the Laplace-Carson transform on expression (19), we obtain the operator conductivity in the form of a rational function

$$Y_{11}(p)=C_0-\sum_{i=1}^{n}\frac{C_i p}{p-p_i}= \\ =\frac{a_{n-1}p^{n-1}+\ldots+a_1 p+a_0}{p^n+b_{n-1}p^{n-1}+\ldots+b_1 p+b_0}. \tag{20}$$

The realizability of function (20) by an electrical circuit does not require proof, since it is obtained as a representation of a sum of exponential curves, and this is characterized by electrical circuits.

The structure of the circuit which realizes function (20) can be chosen arbitrarily.

Let us take the circuit in accordance with physical considerations, i.e., in accordance with system of equations (15) (Fig. 5a). In this, the parameter M, which stipulates the flux in the steel, will be isolated

by a separate branch. This allows, when necessary, the variation in M to be taken into account easily when the steel is saturated. The number of contours must be equal to the exponent of the denominator of expression (20). It is easily verified that in this case we obtain for the circuit (Fig. 5a) an expression for the operator conductivity $Y_{11}^{e}(p)$ of the form of (20)

$$Y_{11}^{e}(p)=\frac{a_{n-1}'p^{n-1}+\ldots+a_1'p+a_0'}{b_n'p^n+\ldots+b_1'p+b_0'}= \tag{21}$$
$$=\frac{c_{n-1}p^{n-1}+\ldots+c_1p+c_0}{p^n+d_{n-1}p^{n-1}+\ldots+d_1p+d_0},$$

where

$$c_i=\frac{a_i'}{b_n'},\quad d_i=\frac{b_i'}{b_n'}.$$

The coefficients of p in expression (21) are a combination of the parameters of the circuit.

Our problem is to determine these parameters. By equating (20) and (21), we obtain 2n equations. The circuit (Fig. 5a) has 2n + 1 unknowns. In order to determine the parameters uniquely, one of them must be given or determined indirectly. The parameters are determined most simply if $L_{1\sigma}$ is known. By knowing $r_1 = \frac{1}{C_1}$ and $L_{1\sigma}$, we find, according to (17),

$$pL(p)=Z_{11}(p)-r_1-pL_{1\sigma}. \tag{22}$$

In accordance with this circuit (Fig. 5a), the remaining parameters can be found by decomposing the expression $\frac{1}{pL(p)}$ into simple fractions.

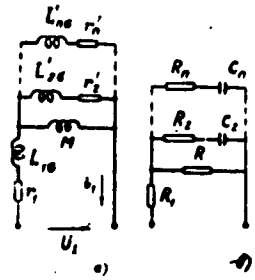

Fig. 5. Equivalent circuit of coil with core (a) and circuit for realization of operator function $L_{11}(p) = L_{1\sigma} + L(p)$ (b)

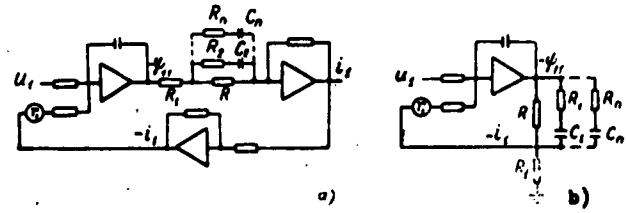

Fig. 6. Circuits of analog of coil with core

In fact, since

$$\frac{1}{pL(p)} = \frac{N(p)}{M(p)} = \sum_{i=1}^{n} \frac{A_i}{p-p_i},$$

where $A_1 = \frac{N(p_1)}{M(p_1)}$, p_1 is the root of the equation $M(p) = 0$, where $p_1 = 0$, then the circuit parameters are determined by the following relations:

$$M = \frac{1}{A_1}, \quad L_{2\sigma}' = \frac{1}{A_2}, \ldots, L_{n\sigma}' = \frac{1}{A_n},$$

$$r_2' = \frac{|p_2|}{A_2}, \ldots r_n' = \frac{|p_n|}{A_n}.$$

Now let us examine the structure of the analog of a coil with core when a computer with solving amplifiers is used.

The equation of the coil was given above (16). Since in this case it is necessary to move from circuits with L and r elements to circuits with R and C elements, let us rewrite Eq. (16) in the form

$$U_1(p) = I_1(p) r_1 + I_1(p) \cdot p[L_{1\sigma} + L(p)]. \tag{23}$$

Let us transform Eq. (23) to a form which is convenient for setting up an analog

$$I_1(p) = \frac{1}{p}\left\{\frac{1}{L_{1\sigma} + L(p)} [U_1(p) - I_1(p) r_1]\right\}. \tag{24}$$

The operator expression in the denominator of (24) is realized by a circuit (Fig. 5b) where

$$R \equiv M, \quad R_1 \equiv L_{1\sigma}, \ldots R_n \equiv L_{n\sigma}',$$

$$C_2 \equiv \frac{1}{r_2'}, \ldots, C_n \equiv \frac{1}{r_n'}.$$

The values of the parameters of the circuit (Fig. 5b) in a concrete case are also functions of the scales selected. In accordance with Eq. (24) let us set up analog circuits of a coil with core (Fig. 6).

Note that an electrical circuit which realizes operator expression (20) can be obtained directly by decomposition of (20) into simple fractions. This circuit will represent a parallel connection of n branches with L and r. The number of parameters of this circuit

equals 2n; therefore, the problem of determining the parameters in this case has a unique solution. In this circuit, however, it is difficult to take saturation into account.

Saturation is taken into account in the circuits (Fig. 6) by the methods described in the examination of the analog of a synchronous machine.

Appendix 2

Decomposition of an Experimental Transient Response Curve into a Sum of Exponential Curves

Curves of stable processes having a monotonic character can be represented as a sum of exponential curves with real, negative exponents. There are several methods for determining the initial ordinates and exponents of the exponential curves. The graphic method has long been known. It consists of replotting the curve on a semi-logarithmic scale [6, 5]. The accuracy of this method is determined by the accuracy with which the graph is constructed.

The essence of the method is as follows. The exponential curves decrease with time, and after a definite time t, it can be assumed that one of them will remain with the lowest exponent in absolute value. If the exponential curve $x_1 = C_1 e^{p_1 t}$ is plotted in a semi-logarithmic scale, then a straight line is obtained

$$\ln x_1 = \ln C_1 + p_1 \cdot t.$$

The intercept of the straight line on the ordinate axis gives $\ln C_1$, and the slope of the line gives p_1.

If the curve of $x(t)$ under study is plotted in the scale of $\ln x = \varphi_1(t)$, then after a time it will be a straight line. Having

found C_1 and p_1, let us find the first exponential curve. Then, subtracting the exponential curve obtained from x(t), let us again plot the function obtained in semi-logarithmic scale

$$\ln(x - C_1 e^{p_1 t}) = \varphi_2(t).$$

Having determined C_2 and p_2, let us find the third exponential curve, etc.

There is still another method for decomposition of a curve into a sum of exponential curves [10]. This accurate analytic method requires that the number of exponential curves be given beforehand, and is more difficult.

The first method can be used for most practical problems.

Appendix 3

An Experimental Check of Analog Based on Experimental Dynamic Characteristics

In order to check the method described above, an analog of a sailient-pole synchronous motor (SM) was made with a power of 7kva, U_{nom} = 220 v, I_{nom} = 18.5 a, n_{nom} = 1000 rpm, T_m = 1035 relative units, with massive poles, and fed from line voltage. The load on the SM was a d-c generator (DCG) with a power of 19 kw, U_{nom} = 220 v, I_{nom} = = 87 a, n_{nom} = 1050 rpm. Transients were studied with a sharply variable load of the DCG. The results of the study on the experimental apparatus were compared with the calculation by the analog. Oscillographs were made of the current of the DCG, the stator current of the SM, and the angle δ with a load on the experimental apparatus. The momentum of the shaft of the SM was determined by the current of the DCG. Then the characteristics $i_d(t)$ and $i_q(t)$ (Fig. 7a) were read

from the SM, which, with decomposition into a sum of exponential curves (Appendix 2), have the following expressions (reduced to $u_d = u_q = 1$):

$$i_d(t) = 1{,}15e^{-1{,}5t} + 3{,}73e^{-0{,}6t} + 1{,}15e^{-0{,}3t} + 0{,}1e^{-0{,}0054t},$$
$$C_{0d} = \Sigma C_{id} = 6{,}13,$$
$$i_q(t) = 8{,}4e^{-0{,}242t} + 1{,}6e^{-1{,}06t},$$
$$C_{0q} = \Sigma C_{iq} = 10.$$

Here the coefficients and exponents are expressed in relative units. Therefore,

$$Y_d(p) = 6{,}13 - \frac{1{,}15p}{p+1{,}5} - \frac{3{,}73p}{p+0{,}6} - \frac{1{,}15p}{p+0{,}3} - \frac{0{,}1p}{p+0{,}0054} = \frac{4{,}28p^3 + 6{,}32p^2 + 1{,}66p + 0{,}00895}{p^4 + 2{,}4p^3 + 1{,}54p^2 + 0{,}278p + 0{,}00146}.$$

Then let us proceed as in Appendix 1. Let us find $px_{ad}(p)$

$$px_{ad}(p) = Z_d(p) - r_k - px_\sigma = \frac{1}{Y_d(p)} - 0{,}163 - 0{,}1p = \frac{0{,}572p^4 + 1{,}07p^3 + 3{,}44p^2 + 0{,}006p}{4{,}28p^3 + 6{,}32p^2 + 1{,}66p + 0{,}00895},$$

where $x_\sigma = 0.1$ is determined by an additional experiment [11]; and $r_k = 0.163$ is the resistance of the contour when reading the characteristic $i_d(t)$.

Let us decompose $\frac{1}{px_{ad}(p)}$ into simple fractions

$$\frac{1}{px_{ad}(p)} = \frac{1{,}49}{p} + \frac{4{,}3}{p+0{,}0185} + \frac{1{,}77}{p+1{,}468} + \frac{0{,}83}{p+0{,}402}.$$

Having proceeded similarly with the curve of $i_q(t)$, we obtain

$$\frac{1}{px_{aq}(p)} = \frac{4{,}08}{p} + \frac{1{,}875}{p+1{,}005}.$$

Circuits for $x_d(p) = x_\sigma + x_{ad}(p)$ and $x_q(p) = x_\sigma + x_{aq}(p)$ are given in Figs. 8a and b. The oscillogram of e(t) for the machine under no-load

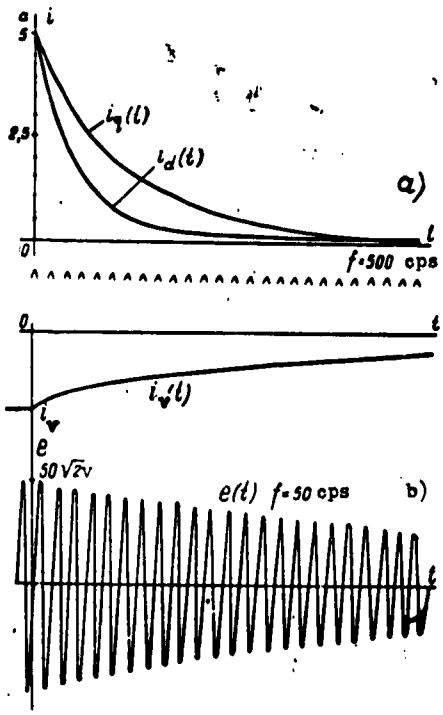

Fig. 7. a) Curves of $i_d(t)$ and $i_q(t)$ in stator of fixed machine when the stator winding is shunted; b) curves of $e(t)$ and $i_v(t)$ in machine running under no-load conditions ($\omega = 1$) when the field coil is shunted.

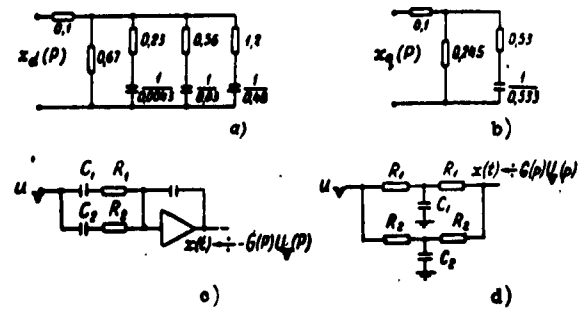

Fig. 8. Circuits for realization of the functions $x_d(p)$, $x_q(p)$, $G(p)$ of a 7-kva synchronous motor.

conditions and with the field coil shunted (Fig. 7b) allows the function $\psi_d(t)$ to be constructed, and then (at $u_v = 1$) $G(p)$. The function $G(p)$, by decomposition into simple fractions, gives the parameters of the equivalent circuit (Fig. 8c and d):

$$\psi_d(t) = 130(0{,}861e^{-0{,}00475t} + 0{,}139e^{-0{,}0532t}),$$

$$C_0 = 130;$$

$$G(p) = \frac{1{,}5p + 0{,}0325}{(p + 0{,}00475)(p + 0{,}0532)} = \frac{A_1}{p - p_1} + \frac{A_2}{p - p_2} = \frac{0{,}524}{p + 0{,}00475} + \frac{0{,}976}{p + 0{,}0532}.$$

The values of the parameters are determined by the formulas:

for the circuit in Fig. 8c

$$R_1 \equiv \frac{1}{A_1}, \quad R_2 \equiv \frac{1}{A_2}, \quad C_1 \equiv \frac{A_1}{|p_1|},$$

$$C_2 \equiv \left|\frac{A_2}{p_2}\right|;$$

for the circuit in Fig. 8d

$$R_1 \equiv \frac{|p_1|}{2A_1}, \quad C_1 \equiv \frac{4A_1}{p_1^2},$$

$$R_2 \equiv \frac{|p_2|}{2A_2}, \quad C_2 \equiv \frac{4A_2}{p_2^2}.$$

The circuit (Fig. 1) with the obtained equivalent circuits for realization of $x_d(p)$, $x_q(p)$ and $G(p)$ was set up on a type-MNM analog, and the same regimes were studied as on the experimental apparatus. Fig. 9 shows oscillograms obtained from the actual machine and from the analog. The nature of the curves is the same. The slight deviation between the experimental and calculated curves can be explained as follows:

1. Saturation of the steel was not taken into account in the analog. At great departures of the angle δ owing to the strong demagnetizing force of the armature, the flux ψ_d decreases, and, therefore, the effect of saturation at these times is small, and the correspondence of the curves is better.

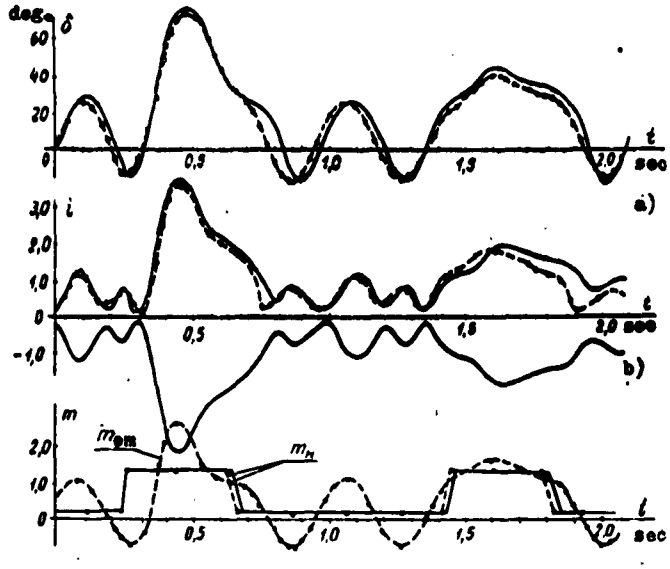

Fig. 9. Oscillograms of transient of synchronous motor with a sharply variable load (———— experiment, — . — . — calculation by analog). a) curves of $\delta(t)$; b) envelope of current of phase a and curve of current obtained with analog by the relation $i = \sqrt{i_d^2 + i_q^2}$; c) moment of load and electromagnetic moment from the relation $m_{em} = \psi_d i_q - \psi_q i_d$.

2. On the analog the moment of the load was set manually, and, therefore, there was no complete correspondence with the curve of the moment on the experimental apparatus. Owing to this, a shift of the curves along the time axis is noted.

3. The MNM analog gives a considerable error, due to the poor operation of the multiplier units. In individual cases this error reached 5%.

The maximum error in the calculation is 8%, which is sufficient for practical purposes.

Various laws of control of excitation (by current, voltage, reactive power, etc.) can be studied on the analog. Thus it is possible to synthesize an excitation regulator and determine its parameters. If it is necessary to take the inertia of the exciter into account, it can be simulated by a separate circuit, or the transient response from the field coil of the exciter to the stator winding $G(p)$ can be obtained experimentally. Then Eq. (8) takes the form

$$\Psi_d(p) = G_v(p)U_{vv}(p) + I_d(p)x_d(p),$$

where $U_{vv}(p)$ is the transform of the voltage on the field coil of the exciter.

The analog of the synchronous motor can be used to study the effect of the load on dynamic stability, which is of interest, for example, when choosing a motor for a sharply variable load.

REFERENCES

1. I. P. Bolyayev. Mathematical Analogs of Circuits of D-C Electrical Machines, Elektromekhanika, No. 1, 1958.

2. N. Kh. Sitnik. Mathematical Analogs of Collectorless A-C Electrical Machines, Elektromekhanika, No. 1, 1958.

3. I. A. Gruzdev and Levinshteyn. The Use of Continuous Action Mathematical Machines for Studying Transients in Electrical Systems, Elektrichestvo, No. 3, 1960.

4. V. S. Tarasov, A. I. Vazhnov, Yu. V. Rakitskiy, V. V. Popov and L. N. Semenova. A Method for Studying Dynamic Stability on Continuous Action Mathematical Machines, Elektrichestvo, No. 4, 1960.

5. Ye. Ya. Kazovskiy. Determining Transients in A-C Machines by Using Frequency Characteristics, Elektrichestvo, No. 4, 1960.

6. M. P. Simoyu. Determining Transient Response by the Time Characteristics of Linearized Systems, Priborostroyeniye, No. 3, 1958.

7. Ya. Z. Tsypkin, Determining the Dynamic Parameters of Systems Described by Linear Differential Equations on Not Above the Second Order by Oscillograms of the Transients, Trudy VZEI, Issue 6, Elektrotekhnika, GEI, 1955.

8. K. P. Kovacs. Messung der gessätigten Werte der synchronen Längs und Querreaktanzen im Stillstand. E und M, 1957.

9. I. I. Sokolov, Yu. Ye. Gurevich and Z. G. Khvoshchinskaya. Modeling of Multi-Generator Systems with a Continuous Action Mathematical Machine, Elektrichestvo, No. 5, 1961.

10. K. Lantsosh. Practical Methods of Applied Analysis, GIFML, Moscow, 1961.

11. V. S. Kulebakin. Testing Electrical Machines and Transformers, 1935.

Submitted November 30, 1961

CALCULATING "SINE" WINDINGS OF SINGLE-PHASE ASYNCHRONOUS MICROMACHINES

K. V. Pavlov and G. S. Somikhina

The basic theoretical prerequisites for sine windings of single-phase asynchronous micromachines were enunciated in an article by the authors [1].

The present article is devoted to calculating "sine" windings, a process with a number of peculiarities in comparison with windings of the ordinary type. These peculiarities are connected with calculating the winding coefficients, with the choice of a favorable distribution of the conductors among the slots, with the calculation of resistance and inductive reactance, etc.

In order to calculate the sine winding the basic initial data must be known: 1) nominal values (power, voltage, current), 2) number of slots in the stator (rotor) z, 3) number of poles 2p, 4) dimensions and shapes of the slots.

Calculating Winding Coefficients

While the calculation of winding coefficients for windings of the usual distribution is done from rather simple known formulas, that of

windings composed of coils of an uneven number of turns is considerably more complex.

In its general form the winding coefficient may be defined as the ratio of the amplitude of the ν-th harmonic of the magnetizing force at the chosen wire distribution in the slots $F_{m\nu}$ to the amplitude of the same harmonic in the so-called "concentrated" wire distribution $F_{mc\nu}$ [1]. By "concentrated" distribution we should understand that provisory distribution in which all the wires comprising part of the winding in two polar divisions are connected in one "diametrical" winding in two slots at a distance of a pole division τ.

The winding coefficient for the ν-th harmonic is

$$k_{o\nu} = \frac{F_{m\nu}}{F_{mc\nu}} , \qquad (1)$$

where $F_{m\nu}$ and $F_{mc\nu}$ are determined by integrating the curves of the magnetizing force constructed for the chosen and for the "concentrated" distribution of wires in the slots

$$k_{o\nu} = \frac{\frac{4}{\pi}\int_0^{\frac{\pi}{2}} f(x)\sin \nu x dx}{\frac{4}{\pi}\int_0^{\frac{\pi}{2}} f_c(x)\sin \nu x dx}, \qquad (2)$$

where $f(x)$ is the curve of the magnetizing force for the chosen wire distribution and $f_c(x)$, that for the "concentrated" wire distribution.

The transformed expression $k_{o\nu}$ [1] has the form:

$$k_{o\nu} = \frac{f(x_0) + \sum_{x_n} \Delta f(x_n)\cos \nu x_n}{f_c(x)}, \qquad (3)$$

where

$$0 \leqslant x_n < \frac{\pi}{2} .$$

In this formula the value of $f(x_0)$ and of the incremental function

$\Delta f(x_n)$ is determined from the spatial curve of the magnetizing force for the corresponding abscissa $\underline{x}$ (Figs. 1 and 2). Abscissa $\underline{x}$ may be determined from the formulas:

with an uneven number of slots per pole τ_z (Fig. 1),

$$x_n = \frac{2np}{z}\pi = \frac{n\pi}{\tau_z}, \qquad (4)$$

where n = 1, 2, 3..., a $x_o = 0$;

with even τ_z (Fig. 2),

$$x_n = \frac{(2n-1)p\pi}{z} = \frac{(2n-1)\pi}{2\tau_z}, \qquad (5)$$

where n = 1, 2, 3..., and $x_o = 0$.

In these formulas $\tau_z = \frac{z}{2p}$ is the number of slots in a pole division; $\underline{z}$ is the total number of stator slots; and 2p is the number of poles.

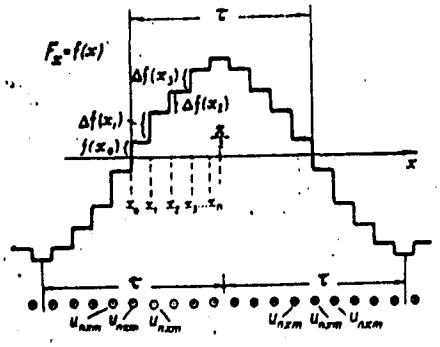

Fig. 1. For determining $k_{o\nu}$ when τ_z is odd.

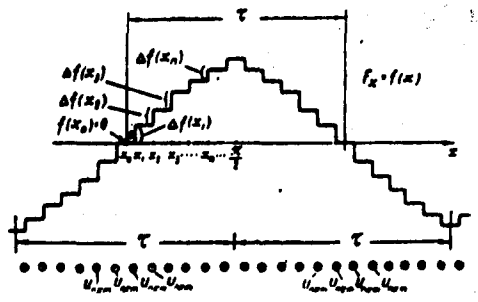

Fig. 2. For determing $k_{o\nu}$ when τ_z is even.

As a starting point for the computation ($x_o = 0$) a point is selected where the magnetizing force curve passes through 0 (Figs. 1 and 2).

If the magnetizing force curve is symmetrical, then abscissa x_n is chosen within the limits 0 to $\frac{\pi}{2}$

$$0 \leqslant x_n < \frac{\pi}{2}.$$

In "concentrated" distribution the magnetizing force curve will have a rectangular shape (Fig. 3) and $f_c(x)$ represents the height of the rectangle.

The number of conductors in the slot occupied by the provisory "diametrical" coil, u_{nc}, will equal the total number of conductors in the slots of one pole division

$$u_{nc} = \sum_{\tau} u_{nx}, \tag{6}$$

and the magnetizing force of $f_c(x)$ is composed of the ordinate of $f(x_0)$ and the sum of the increments $\Delta f(x_n)$ (Figs. 1,2)

$$f_c(x) = f(x_0) + \sum_{x_n} \Delta f(x_n), \tag{7}$$

where

$$0 < x_n < \frac{\pi}{2}.$$

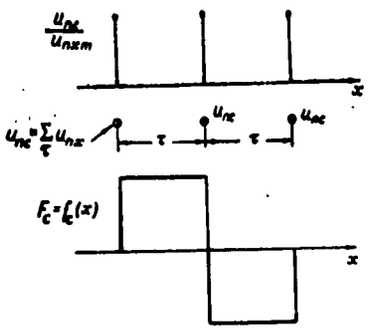

Fig. 3. "Concentrated" placement of conductors in two pole divisions in a "diametrical" coil.

Consequently the winding coefficient formula for the ν-th harmonic may be presented in the form

$$k_{0\nu} = \frac{f(x_0) + \sum_{x_n} \Delta f(x_n) \cos \nu x_n}{f(x_0) + \sum_{x_n} \Delta f(x_n)}, \tag{8}$$

where

$$0 < x_n < \frac{\pi}{2}.$$

Selecting Favorable Winding Conductor Distribution Among the Slots

The law for distributing the conductors among the slots must be selected in such a way as to secure the greatest approximation of the three-dimensional curve of the magnetizing force to the sinusoid. In addition the actual performing of the winding should not be made too complicated.

It is a practical impossibility to suppress all the higher harmonics in the curve of the magnetizing force in the case of windings distributed among slots. Therefore it is desirable to suppress the third harmonic and weaken the fifth and seventh harmonics in approximating the curve of the magnetizing force of single-phase asynchronous machines to the sinusoid.

The general condition for suppressing the ν-th harmonic is setting its winding coefficient equal to zero

$$k_{o\nu} = \frac{f(x_o) + \Sigma \Delta f(x_n) \cos \nu x_n}{f_c(x)}$$

Hence

$$f(x_o) + \Sigma \Delta f(x_n) \cos \nu x_n = 0 \qquad (9)$$

for $$\nu \neq 1.$$

The condition for suppressing the third and weakening the fifth and seventh harmonic will be written thus:

$$f(x_o) + \Sigma \Delta f(x_n) \cos 3x_n = 0 \qquad (10)$$

when $$k_{o5} \to 0 \text{ and } k_{o7} \to 0.$$

It is possible in practice to choose a law for conductor distribution among the slots (at given numbers of slots and poles) such that the above indicated Conditions 9 or 10 are satisfied. One of the most favorable distribution laws is the "curvilinear trapezoid" law, in which one third of the slots in a pole division is filled with the maximum number of conductors of a given phase of the winding and in the remaining slots of the pole division the number of conductors gradually decreases to a certain minimum value.

The condition for fulfilling this law is

$$\frac{\tau_z}{3} = \text{a whole number}, \qquad (11)$$

where τ_z is the number of slots per pole division.

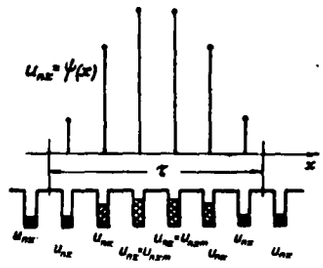

Fig. 4. Distribution of conductors among slots according to the "curvilinear trapezoid" law with maximum filling of $\frac{\tau_z}{3}$ slots.

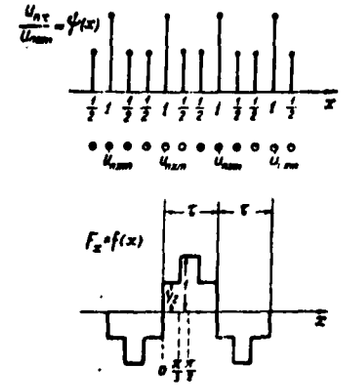

Fig. 5. Variant in conductor distribution among slots when $\tau_z = 3$.

Figure 4 shows an example of the $u_{nx} = \psi(x)$ distribution. At the minimum number of slots $\tau_z = 3$ the "trapezoid" conductor distribution degenerates into the "triangular." In this the higher harmonic content of the curve of the magnetizing force remains considerable (see Table 1 and Fig. 5).

The larger the number of slots per pole, the more possibilities there are of approximating the spatial curve of the magnetizing force to the sinusoid.

Filling one third of the slots in a pole division with the maximum number of conductors is not in itself enough to produce a favorable shape in the curve of magnetizing force. Doing this also depends on the distribution of the conductors in the remaining slots of the pole division.

The suitability of this or that law of conductor distribution among the slots is estimated from the value of the winding coefficients of the higher harmonics.

TABLE 1

Winding Coefficients Of Single-Phase Sine Winding For Certain Favorable Variants.

Variant No.	t_z	Conductor distribution among slots and shape of curve of magnetizing force	Winding coefficient formula	Numerical values of winding coefficients			
				k_{01}	k_{03}	k_{05}	k_{07}
1	3*	Fig. No. 5	$k_{0\nu} = \frac{1}{2} + \frac{1}{2}\cos\nu\frac{\pi}{3}$	0,75	0	0,75	0,75
2	6	Fig. No. 6	$k_{0\nu} = \frac{3}{8}\cos\nu\frac{\pi}{4} + \frac{1}{2}\cos\nu\frac{\pi}{12} + \frac{1}{8}\cos\nu\frac{5\pi}{12}$	0,78	0	0,0145	0,0145
3	9	Fig. No. 7	$k_{0\nu} = \frac{1}{6} + \frac{1}{3}\cos\nu\frac{\pi}{9} + \frac{5}{18}\cos\nu\frac{2\pi}{9} + \frac{1}{6}\cos\nu\frac{\pi}{3} + \frac{1}{18}\cos\nu\frac{4\pi}{9}$	0,785	0	0,025	0,018
4	12	Fig. No. 8	$k_{0\nu} = \frac{1}{4}\cos\nu\frac{\pi}{24} + \frac{1}{4}\cos\nu\frac{\pi}{8} + \frac{7}{32}\cos\nu\frac{5\pi}{24} + \frac{5}{32}\cos\nu\frac{7\pi}{24} + \frac{3}{32}\cos\nu\frac{9\pi}{24} + \frac{1}{32}\cos\nu\frac{11\pi}{24}$	0,787	0	0,029	0,0133

*When $\tau_z = 3$ the trapezoid law degenerates into the triangular.

Table 1 lists the formulas and values of the winding coefficients

for several favorable variants of the "trapezoid" distribution of the conductors presented in Figs. 5-8.

Distribution of Number of Winding Turns Among the Coils

In windings of the "sine" type the conductors of both windings are distributed among all the slots in conformity with the chosen law. In this type there appear in each slot (or in the majority of them) conductors belonging to both the main and auxiliary winding. Thus, when the main winding is arranged in the slots room must be set aside for the auxiliary one, too.

As indicated above, the coils of the sine winding have various dimensions and various numbers of turns. The number of coils of the same size depends on the number of poles and slots.

There are two coils of the same size for each pair of poles. Besides that, when τ_z is odd there are supplementary coils: either one large coil with w_{k_o} turns or (when $2p > 2$) two half coils with $\frac{w_{ko}}{2}$ turns in each. The schematics of sine windings with even and odd τ_z are shown in Figs. 9 and 10.

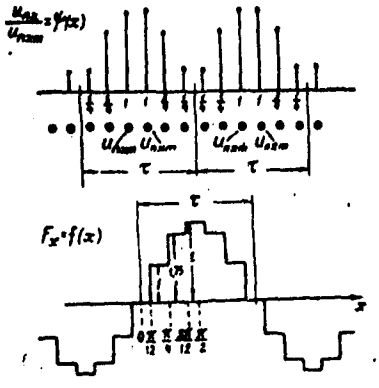

Fig. 6. Favorable variant of conductor distribution among the slots when $\tau_z = 6$.

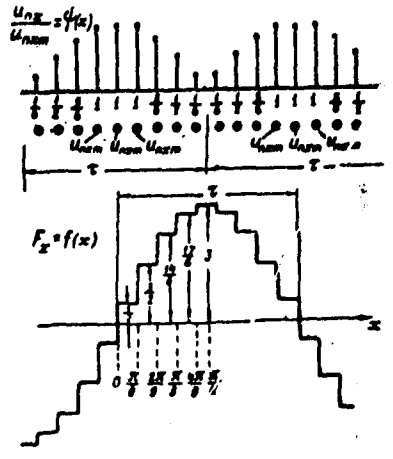

Fig. 7. Favorable variant of conductor distribution among the slots when $\tau_z = 9$.

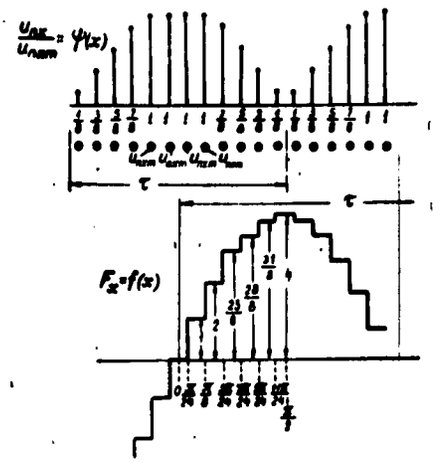

Fig. 8. Favorable variant of conductor distribution among the slots when $\tau_z = 12$.

The number of coils for main winding N_{kn} and their number of turns w_{kv} may be found if we calculate the winding coefficient of the first harmonic for the selected distribution and find the number of winding turns

$$w_{kA} = \frac{U_1}{4{,}44 \cdot f_1 \cdot k_{01} \cdot \Phi}. \qquad (12)$$

The total number of coils in the winding when τ_z is even is

$$N_{kA} = N_{k_1} + N_{k_2} + N_{k_3} + \ldots + N_{kn} = p\tau_z, \quad (13)$$

and when τ_z is odd,

$$N_{kA} = N_{k_0} + N_{k_1} + N_{k_2} + N_{k_3} + \ldots + N_{kn} = N_{k_0} + p(\tau_z - 1) \quad (14)$$

Here N_{k_1} is the number of coils of maximum size with maximum number of turns $w_{k_1} = w_{km}$; N_{k_2}, N_{k_3}, etc. are the numbers of coils of lesser dimensions corresponding to winding numbers w_{k_2}, w_{k_3}, etc. $N_{k_0} = p$ is the number of supplementary coils with w_{k_0} turns when τ_z is odd; $N_{k_0} = 2p$, if half-coils with $\frac{w_{k_0}}{2}$ turns are made. The number of turns in any coil is

$$w_{kx} = \psi_x w_{km}, \qquad (15)$$

where $\psi_x = \frac{u_{nx}}{u_{nxm}}$ is the relative filling of a slot with turns of a given coil and w_{km} is the number of turns in the largest coil.

The entire number of turns in the main coil is;

when τ_z is odd

$$w_{sA} = N_{k_0}\psi_o w_{km} + N_{k_1}\psi_1 w_{km} + N_{k_2}\psi_1 w_{km} + \ldots + N_{kn}\psi_n w_{km}, \qquad (16)$$

when τ_z is even

$$w_{xA} = N_{k_1}\psi_1 w_{km} + N_{k_2}\psi_2 w_{km} + \ldots + N_{kn}\psi_n w_{km}. \qquad (17)$$

From these expressions w_{km} is determined and then the numbers of turns in all the coils, taking ψ_x into consideration.

The relative filling of a slot with conductors of the auxiliary winding ψ_{xB} should also be expressed in fractions of the number of conductors in a slot filled to the maximum by the main winding u_{nxmA}. The total filling of the slots with conductors of the main and auxiliary windings ψ_{xAB} in relative units may be determined from the formula

$$\psi_{xA} = \psi_{xA} + \psi_{xB} = \frac{u_{nxA} + u_{nxB}}{u_{nxmA}} \qquad (18)$$

ψ_{xAB} in all slots must be as nearly the same as possible and satisfy the condition $k_{fan} \leqslant 0.7$.

At the admissible coefficient of slot filling ($k_{fan} = 0.65$ to 0.7) we may determine the relative numbers of conductors of the auxiliary coil in the different slots ψ_{xB}.

The coefficient of slot filling by conductors of both windings may be expressed as

$$k_{fan} = \frac{d_A^2 u_{nxA} + d_B^2 u_{nxB}}{S'_n} \leqslant 0.7, \qquad (19)$$

where d_A, d_b are the diameters of the insulated wire of the main and auxiliary windings chosen in conformity with the given current density in the windings

$$\frac{d_{A^2}}{d_{B^2}} \approx \frac{\Delta_B}{\Delta_A} = t, \qquad (20)$$

S'_n is the area of the slot not considering insulation and taper.

From Formula 19 (taking Formula 20 into consideration) we find

$$u_{nxA} + \frac{u_{nxB}}{t} = \frac{k_{fan} S'_n}{d_{A^2}} \qquad (21)$$

In relative units this expression takes the form

$$\psi_{xA} + \frac{\psi_{xB}}{t} = \frac{k_{fan} S_n'}{d_A^2 u_{nxmA}}. \qquad (22)$$

Hence the relative number of auxiliary winding conductors in any slot will be

$$\psi_{xB} = \left(\frac{k_{fan} S_n'}{d_A^2 u_{nxmA}} - \psi_{xA} \right) t. \qquad (23)$$

The computation of the number of coils and turns in the coils of the auxiliary winding should be made from the discovered values of ψ_{xB}, just as in the main winding.

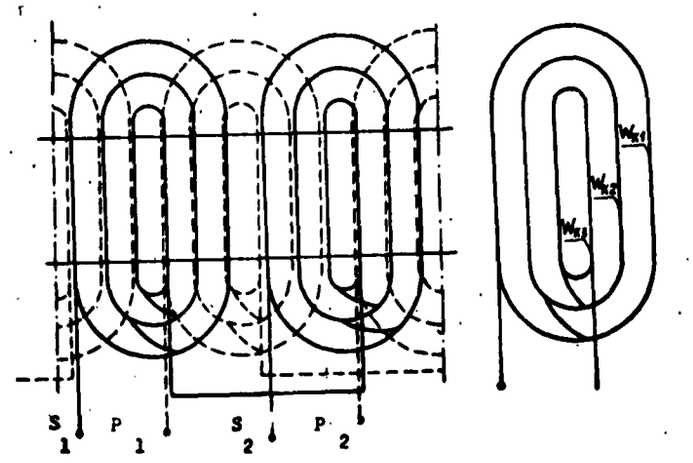

Fig. 9. Diagram of sine winding with τ_z even.

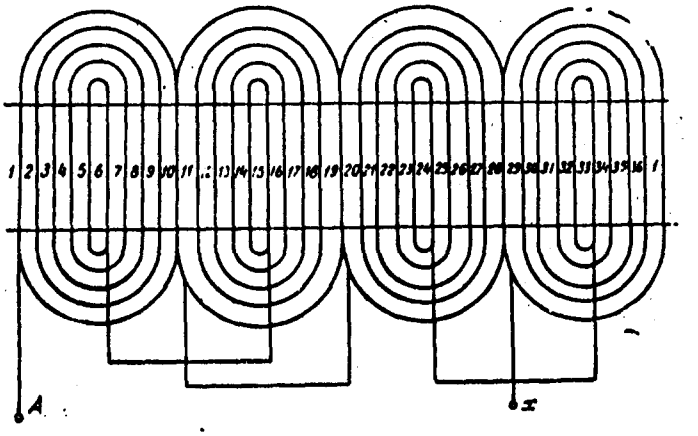

Fig. 10. Diagram of sine winding with τ_z odd.

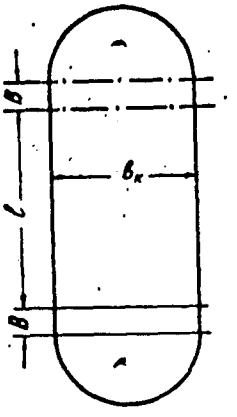

Fig. 11. To determine length of end of coil.

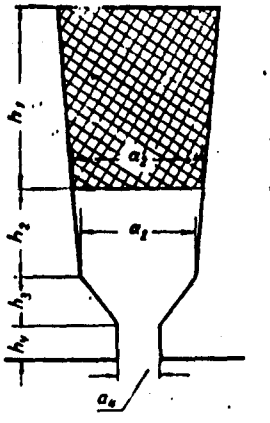

Fig. 12. To determine coefficient of permeance of slot leakage.

Calculating Winding Resistance

The calculation of the resistance and inductive reactance of the main and auxiliary windings also has a number of peculiarities.

The total length of the conductor in all the coils of the windings may be defined as

$$\Sigma L_{kx} = L_{k_1} + L_{k_2} + L_{k_3} + \ldots + L_{kn}, \qquad (24)$$

where the length of the conductor in a coil of a definite size is

$$L_{kx} = 2(l + l_{ex}) w_{kx} \cdot 10^{-2} \text{ m} \qquad (25)$$

Here l is the length of the stator pack in centimeters; l_{ex} is the length of the end part of a coil of a definite size

$$l_{ex} = 0.5\pi b_{kx} + 2B, \qquad (26)$$

where b_{kx} is the width of a coil of a definite size and B is the "straight" region of the end part (Fig. 11).

The resistance of the main (or auxiliary) winding is

$$r_s = \rho \frac{\Sigma L_{kx}}{Sa}. \qquad (27)$$

Here a is the number of parallel arms and S is the cross section of the wire (mm^2).

The inductive reactance of the leakage of the sine windings must not be computed from the formulas used for windings of the ordinary type because the filling in of the individual slots is not the same, but the coils have different sizes and shapes.

An exact calculation of the leakage of the sine windings is very complicated. The following formulas may be used for practical computations of the inductive reactance of the leakage of the sine windings.

The inductance of the coil caused by slot leakage is

$$L_{sxn} = 2w_{kx}^2 \mu_0 \lambda_{nx} l. \qquad (28)$$

When all coils are sequentially connected the inductance of the slot leakage of the winding is

$$L_{sn} = \Sigma L_{sxn} = 2\mu_0 l \Sigma N_{kx} w_{kx}^2 \lambda_{nx}. \qquad (29)$$

The coefficient of permeance of slot leakage λ_{nx} is determined for each of the coils from the known formulas, taking the shape of the slot into consideration.

When computing λ_{nx} in sine windings we must allow for the relative filling of the slot with the conductors of the main or auxiliary winding.

It is also necessary to allow for the fact that the main winding is usually placed nearer the bottom of the slot and the auxiliary winding nearer its top.

We determine λ_{nx} in trapezoidal slots (Fig. 12) from these formulas for the main winding,

$$\lambda_{nxA} = \frac{h_1}{3a_2'} + \frac{2h_2}{a_2 + a_2'} + \frac{3h_3}{a_2 + 2a_4} + \frac{h_4}{a_4}, \qquad (30)$$

for the auxiliary winding,

$$\lambda_{nxB} = \frac{h_2}{3a_2} + \frac{3h_3}{a_2 + 2a_4} + \frac{h_4}{a_4}. \qquad (31)$$

In these formulas the heights of the part of the slot occupied by the main winding and the auxiliary winding are h_1 and h_2 respectively and are determined from the relative filling of the slot with the conductors of one or the other winding. The dimensions h_1, h_2, and a_2' may be discovered by graphically representing the slot to scale and dividing its area in the ratio

$$\frac{S_{nA}}{S_{nB}} = \frac{w_{xA}}{w_{xB}} t, \qquad (32)$$

where S_{nA} is the area of the slot occupied by the conductors of the main winding and S_{nB} is its area occupied by auxiliary winding conductors.

The inductive reactance of slot leakage for the whole winding

(main or auxiliary) is

$$x_{sn} = 4\pi\mu_0 f l \Sigma N_{\kappa x} w_{\kappa x}^2 \lambda_{n x} = 1{,}6\pi^2 10^{-8} f l \Sigma N_{\kappa x} w_{\kappa x} \lambda_{n x}. \qquad (33)$$

The inductance of the coil caused by end leakage is

$$L_{sxe} = 2 w_{\kappa x}^2 \mu_0 \lambda_{ex} l. \qquad (34)$$

The total inductance of end leakage of all the coils of a winding is

$$L_{se} = \Sigma L_{sxe} = 2\mu_0 l \Sigma N_{\kappa x} w_{\kappa x}^2 \lambda_{ex} \qquad (35)$$

Here λ_{ex} is the coefficient of permeance of the end leakage of the coil referred to the length of the stator pack.

The coefficient of permeance of the leakage of the end parts λ_{ex} depends on the shape and geometrical dimensions of the end parts of the winding, on the mutual disposition of the coils, etc. Accurate determination of coefficient λ_{ex} is complex and coupled with laborious computation.

Inasmuch as the inductive reactance of the end parts is a relatively small part of the total inductive reactance of the winding it is usually calculated from approximate formulas.

We may, for example, introduce some average coefficient λ_{eav} computed for a coil of average size. This coefficient may be approximately calculated from the formula for the single-phase winding

$$\lambda_{eav} \simeq 0{,}39\left(1 - 0{,}6\frac{Q}{\tau_z}\right)\frac{Q}{l}(l_{eav} - 0{,}64 b_{kav}) \qquad (36)$$

where Q is the number of slots per pole occupied by a winding (main or auxiliary); τ_z, the number of slots per pole; l_{eav}, the length of the end part of a coil of average size (cm); b_{kav}, the width of a coil of average size (cm); and l, the calculated length of the stator (cm).

The inductive reactance of the end leakage in this case will be

$$x_{s\sigma} \cong 1{,}6\pi^2 10^{-8} f l \lambda_{\sigma v} \Sigma N_{sx} w_{sx}^2. \qquad (37)$$

The inductive reactance of the differential leakage is

$$x_{s\partial} = 1{,}58 f \frac{w_{sA}^2 l}{p} \lambda_\partial \cdot 10^{-7} \ (ом), \qquad (38)$$

where

$$\lambda_\partial = \frac{m}{\pi^2} \frac{\tau}{k_1 k_z \delta} \sum_{\nu = 3, 5, 7, 9, 11 \ldots\ldots} \left(\frac{k_{0\nu}}{\nu}\right)^2, \qquad (39)$$

In these formulas λ_∂ is the coefficient of the magnetic conductance of the differential leakage; m = 2, the number of phases for single-phase machines; $\tau = \frac{\pi D}{2p}$, the pole division; δ, the air gap; k_δ, coefficient of the air gap allowing for the slots in the stator computed from generally known formulas; k_z, coefficient of saturation of the magnetic circuit determined from the calculation of the magnetic circuit; ν, the order of the harmonic; $k_{o\nu}$, winding coefficient for the higher harmonics calculated for a number of odd harmonics by the above described method.

Thus we may recommend the following order in computing a single-phase sine winding.

1. First, we choose the distribution of the conductors of the main winding among the slots in relative units $u_{nxA} = \psi(x)$. In this, one third of the slots of a pole division is filled with the maximum number of main winding conductors u_{nxmA}. In the remaining slots the law of decreasing the number of conductors may at first be assumed to be linear.

The law of the distribution of the conductors of the auxiliary winding $u_{nxB} = \psi(x)$ may be the same as in the main winding, but the displacement of the axes of the windings by $\frac{\tau_z}{2}$ is allowed for.

2. The winding coefficients are calculated for the preliminarily chosen law of distribution of conductors among the slots for the main and auxiliary winding in order to estimate the favorability of the selected law.

3. The optimum distribution is found according to the optimum condition

$$k_{o3} = 0;\ k_{o5} \to 0;\ k_{o7} \to 0.$$

When choosing the optimum variant we may use Table 1 which lists some examples of favorable distribution among the slots for different τ_z and numerical values of winding coefficients in these cases.

4. After having calculated the winding coefficient of the first harmonic k_{o1} for the adopted law of conductor distribution we determine the entire number of turns for the main phase.

5. Since in the same laws of conductor distribution among the slots in the main and auxiliary winding the winding coefficients are the same ($k_{o1A} = k_{o1B}$), the number of turns in the auxiliary winding is determined from the given coefficient of transformation

$$w_{sB} = kw_{sA}.$$

6. The schematics of the main and auxiliary winding are drawn up.

7. The number of coils of different sizes N_{kxA} and the number of turns in each coil w_{kxA} of the main winding are determined.

8. The relative number of conductors in the auxiliary winding ψ_{xB} is discovered.

9. The total filling of all slots by conductors of the main and auxiliary coils ψ_{xAB} is verified.

10. The number of coils N_{kxB} and the number of turns in these coils w_{kxB} of the auxiliary winding are calculated.

11. The resistance and inductive reactance of the main and auxiliary winding are determined.

REFERENCES

1. G. S. Somikhina and K. V. Pavlov. Distributed Single-Phase "Sine" Windings of Asynchronous Micromachines, Elektromekhanika, No. 11, 1958.

2. R. Rikhter. Armature Windings of AC and DC Machines. Energoizdat, 1933.

3. Yu. S. Chechet. Electric Micromachines for Automatic Apparatus. GEI, 1957.

Manuscript received July 11, 1961.

A SINGLE-ARMATURE CONVERTER WITH SUPERIMPOSED MAGNETIZATION

I. S. Kopylov

A reliable and economical frequency converter is necessary in electric drives with frequency control in use in high-speed technological processes of the metal working, textile, and other branches of industry and also in slow-speed drives with high-frequency sources of supply [1].

The most successful converter for frequency control of a-c motors is, in our opinion, the circuit proposed by Academician V. S. Kulebakin [2, 3].

In the Kulebakin circuit a rectified voltage regulated by a saturation choke coil is led from the commutator to the single-armature converter (Fig. 1). A single-armature converter supplied with d-c functions as a d-c motor and as a synchronous generator viewed from the slip-rings. The frequency when it leaves the single-armature converter is proportional to the speed of rotation and the number of poles, but in independent excitation the effective value of the voltage on the slip-rings is proportional to the frequency. Meantime the ratio $\frac{U}{f}$ = const., which is also necessary for the optimum law of frequency control of asynchronous motors.

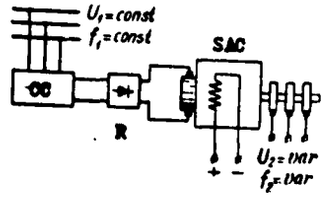

Fig. 1. Academician V. S. Kulebakin's frequency converter circuit: CC) saturation choke coil; R) power rectifier; SAC) single-armature converter; U_1, f_1) circuit voltage and frequency; U_2, f_2) voltage and frequency leaving the converter.

The single-armature converter with superimposed magnetization is a development of the Kulebakin circuit.* In such a converter a magnetic amplifier is combined with the converter and this ensures a decrease in weight and makes possible internal feedback without special windings.

In the single-armature converter with superimposed magnetization (Fig. 2 and 8) the back of the stator is laminated and divided into two toroids on which are wound the a-c windings of the magnetic amplifier ($W_{\sim}$); and the control windings (W_c), shift windings (W_s), and feedback windings (W_f) encompass both toroids while first harmonic induction from the alternating current is lacking in them. On the poles there is the concentrated excitation winding (W_e) and the regulating winding (W_r).

A simple loop winding soldered to the slip-rings, the number of which is determined by the number of phases in the a-c system, is placed on an armature with an even number of poles.

The magnetic amplifier in a single-armature converter may be single-phase or three-phase. The schematic in Fig. 2 shows the magnetic amplifier mounted with internal feedback as an open-circuit bridge. The external feedback winding is small and designed to regulate the amplification factor of the magnetic amplifier.

---

* I. P. Kopylov. Certificate of Authorship No. 118103 of April 25, 1958.

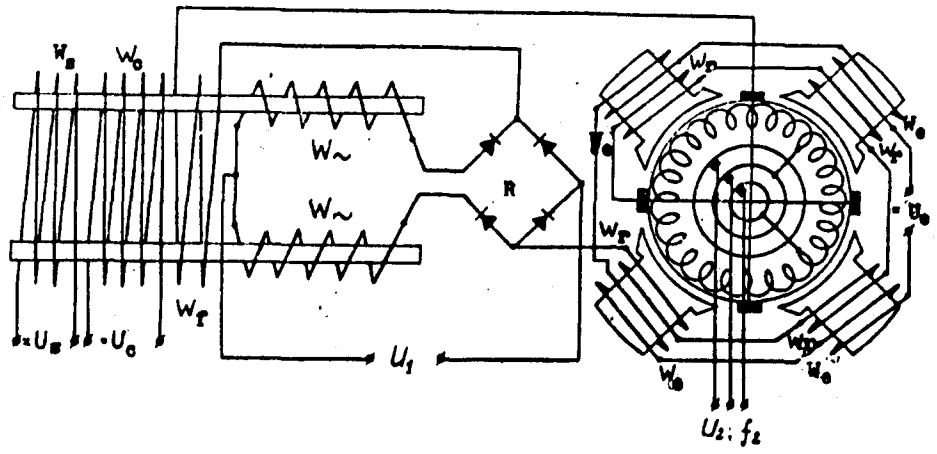

Fig. 2. Single-amature converter with superimposed magnetization. U_e, U_c, U_s are the excitation, control, and shift voltages respectively.

The excitation currents are imposed in the back of the stator on the magnetic amplifier currents and are distributed unevenly along the stator, since where the amplifier and excitation direct currents add together the saturation is greater and where the currents subtract from each other the saturation is less. The effect of the excitation current on the magnetic state of the core is equivalent to a certain shift of the working current and the basic curve of magnetization. The effect of the excitation field on the characteristics is found to be insignificant, since the magnetizing force of the excitation winding compared to the magnetizing force of the control winding turns out to be small.

The effect on the magnetic amplifier's fields is like the same effect in the motor of a direct current amplifier [4].

When the converter has a constant excitation current the input-output curve of the magnetic amplifier, plotted against speed, expresses the converter's speed of rotation and consequently the frequency on the slip-rings.

The ratio of the emf from the a-c (E_2) side and that from the d-c (E_1) side is

$$k_e = \frac{E_2}{E_1} = k_\beta \frac{\sin \frac{\pi}{m}}{\sqrt{2}}, \quad (1)$$

where k_β is the coefficient of field distribution (for the sinusoid $k_\beta = 1$); and m, the phase number.

In the single-armature converter

$$\dot{E}_1 = \dot{U}_c - \dot{U}_{ma} \quad (2)$$

where $\dot{U}_n$ is the voltage of the network; and $\dot{U}_{ma}$, the voltage on the magnetic amplifier (perhaps discovered from a vectorial diagram of the single-armature converter).

The current ratio is the same as in an ordinary converter

$$k_i = \frac{I_{21}}{I_1} = k_\beta \frac{2\sqrt{2}(1-\rho)}{m \cos \varphi}, \quad (3)$$

where I_{21} is the line current from the slip-ring side; and I_1, the current from commutator side.

$$\rho = \frac{P_m}{E_1 I},$$

P_f is the steel and friction losses of the single-armature converter.

The current in the power windings of the magnetic amplifier ($I_\sim$) may be found from known relationships, starting from current I_1. For a two-stage layout the effective value of current $I_\sim = k_f I_1$ (for the sinusoid $k_f = 1.11$).

In a change of signal in the control winding of the magnetic amplifier the voltage on the slip-rings and the frequency change proportionally and this guarantees the constancy of ratio $\frac{U}{f}$.

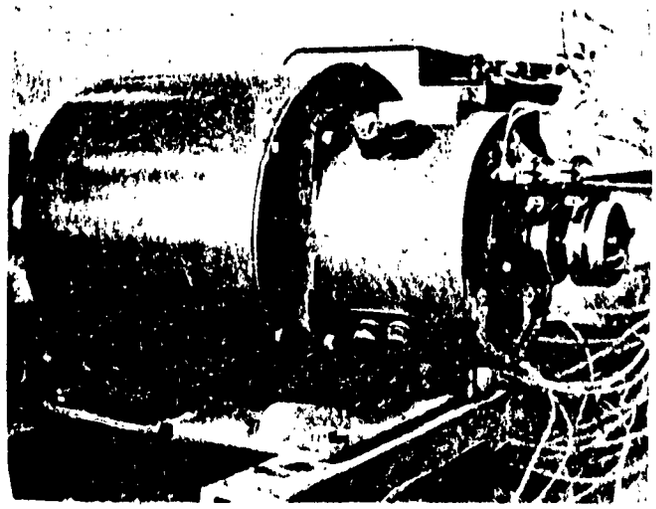

Fig. 3. Experimental single-armature converter with superimposed magnetization.

The current in the sections of the armature winding is equal to the difference between the d-c and the a-c and depends on cos φ of the load. If we assume that losses in the converter armature may be allowed to be the same as when it is functioning as a d-c machine, the power of the converter may be increased by 20 to 30% depending on number of phases and cos φ.

When being fed from the d-c side commutation under transients and on starting is smooth. In another work by the author [5] he points out the feasibility of constructing single-armature converters without additional poles when being powered from the d-c side up to 20-30 kw.

When the converter is working into an asynchronous motor the latter will require reactive power as well as active. Therefore there appears a longitudinal component of the magnetizing force in the a-c of the amature reaction and this component demagnetizes the more, the lower cos φ is. Weakening the excitation field leads to increasing the converter's rotational speed and consequently the frequency on

the slip-rings. Spontaneous feedback is increased by the regulating winding which is consequently cut into the load and has a small number of turns.

We begin the calculation of a single-armature converter with that of the output stage of such a converter figured by known methods and choose only an induction in the stator back on the linear portion of the magnetization curve. Given the geometry of the steel for the converter and the voltage of the power-supply, the amplifier is computed, selecting a number of a-c winding turns so as to secure the minimum distance between the toroids.

In the Moscow Institute of Energetics (MEI) in the electric machine department there was computed and tested a single-armature converter with superimposed magnetization P_2 = 1 kw, $U_\sim$ = 127 v, f = 50 cps, output voltage 110 v, and range of change of 10.1.* The single-armature converter was made on the base of the motor-dc amplifier described in a previously cited work [4] by conducting three leads from its armature winding to the slip-rings (Fig. 3).

Figure 4 shows the relationship of U_2 and $f_2 = \varphi(I_c)$ when $U_\sim$ = = 127 v. With a decrease in cos φ of the load the size of the linear zone increases, explicable by the demagnetizing action of the longitudinal reaction of the a-c armature. When the single-armature converter and the choke are built separately this increase does not occur.

The relationships of U_2, f_2, and also current I_2 to current I_c are congruent with the input-output characteristics of the magnetic amplifier. The current on the constant frequency side (I_1) is an

* Engineer V. A. Poteyenko took part in the work, defending his graduating project on this theme.

exception, the change in which is influenced by the change in both the choke coil and the frequency.

The regulating winding, connected up opposite to the excitation winding, broadens the linear zone somewhat, but this coil must be weak (approximately 15%) of the magnetizing force of the excitation winding, since a powerful regulating winding destroys the stability of the converter's functioning.

Figure 5 gives the relationships of $\frac{U_2}{f_2}$ and $\underline{n}$ of the motor to current I_c when an asynchronous motor is connected to the output of the converter.

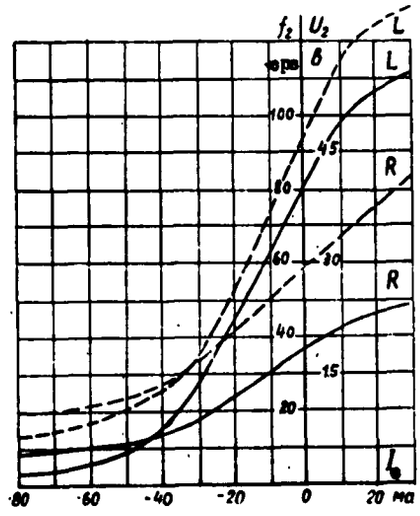

Fig. 4. U_2 and $f_2 = \varphi(I_c)$ when U = const. The dashed line give the change in voltage U_2 – L with an inductive and R with an active load.

$\frac{U_2}{f_2}$ remains almost constant owing to spontaneous feedback between the asynchronous motor load current and the voltage at the choke coil output (feedback between the magnetic amplifier's saturated steel and the current of the armature's longitudinal reaction).

The external characteristics of the single-armature converter with superimposed magnetization U_2, $f_2 = \varphi(I_2)$ when $U_\sim = 127$ v are shown in Fig. 6. The nature of the load influences the form of the external characteristics and the differing effects of the armature reaction explain this. In this process, the frequency noticeably changes as a result of the change in speed, but U_2 alters little because the voltage applied to the armature is almost unchanged.

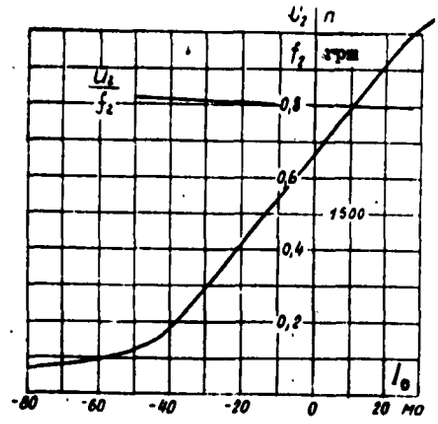

Fig. 5. $\frac{U_2}{f_2}$ and $n = \varphi(I_c)$ when U = const.

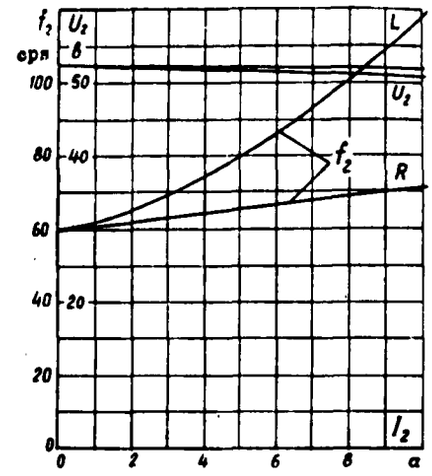

Fig. 6. U_2 and $f_2 = \varphi(I_c)$ when I_c and U_1 = const.

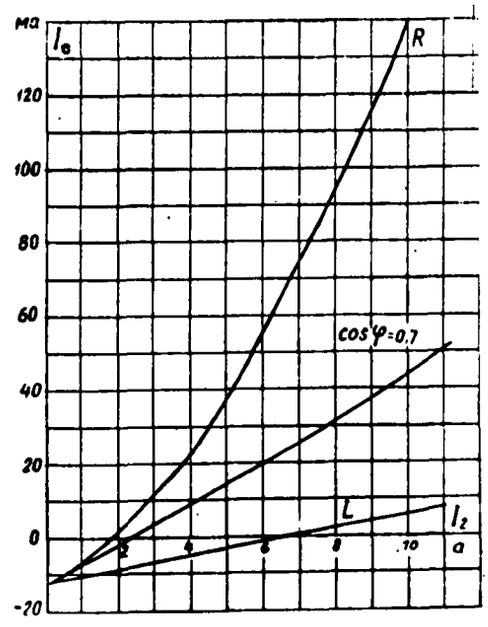

Fig. 7. $I_c = f(I$) when U_2 and U_1 = const.

Figure 7 represents the regulating characteristics of $I_c = f(I_2)$.

The characteristics were noted when the network was under constant voltage, and the output voltage U_2 was kept constant because of the change in the control current.

In frequency regulation the presence of spontaneous feedback

along the load current provides a more favorable course of the transient when this converter is used. When the load is increased on the drive motor the load current increases and the longitudinal reaction of the armature also increases, leading to an increase in the frequency and speed of motor rotation, guaranteeing rigid mechanical characteristics.

The experimental converter guarantees a smooth change in the frequency from 10-12 to 100-120 cps. It is necessary to increase the dimensions of the choke coil and calculate the converter for higher speeds in order to broaden the limits of regulation.

In the normal geometry of the machine we may obtain a frequency change to 400-500 cps. For this the converter, when $2P = 4$, must have a rotational speed of 8000-9000 rpm.

Putting a single-armature converter with superimposed magnetization and an asynchronous frequency converter in the same unit we may obtained a doubled frequency (Fig. 8). In this case, the solder couplings from the armature winding are made to the leads of the phase winding of the rotor and the doubled frequency is taken off the stator. Such a converter has no slip-rings and enables us to derive a frequency of up to 1000 cps. In this variant the converter is convenient for transforming frequencies of 50 cps to higher ones.

The transformation of high frequencies into lower ones also has a certain interest. Single-armature converters with superimposed magnetization may find application for obtaining and smoothly changing low frequency in units with a network frequency of 400 cps. In this case the converter is compact, thanks to the small dimensions of the choke coil.

The single-armature converter with superimposed magnetization cannot guarantee individual frequency regulation or voltage regulation

and can be successfully used only where it is necessary to have constancy in the current, i.e., $\frac{U}{f}$ = const.

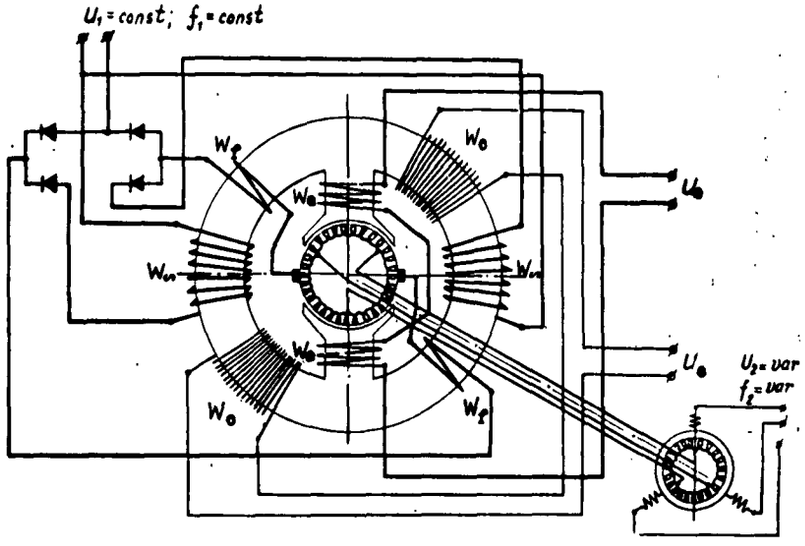

Fig. 8. Schematic of single-armature converter with superimposed magnetization together with asynchronous frequency converter.

Conclusions

The single-armature converter with superimposed magnetization, a single-unit frequency converter, may find successful application in frequency regulation of a-c machines.

Combined construction of the choke coil and the single-armature converter secures a certain decrease in weight because of the decrease in weight of the construction materials and better cooling of the choke-coil windings.

Spontaneous feedback along the current makes it possible to attain better static and dynamic characteristics.

REFERENCES

1. A. A. Bulgakov. Frequency Control of Asynchronous Electric Motors. Izd. AN SSSR, 1955.

2. V. S. Kulebakin. The Use of Semiconducting Rectifiers and Saturated Choke-Coils in the Circuits of Automated Electric Drives. Izd. AN SSSR, OTN, No. 2, 1958.

3. V. S. Kulebakin, and A. A. Yanshin. The Basic Properties of Frequency Regulation of a-c Drives by the Use of Single-Armature Converter. Izd. AN SSSR, OTN, No. 1, 1959.

4. I. P. Kopylov. A d-c Motor Amplifier. Elektrichestvo, No. 1, 1959.

5. M. M. Krasnoshapka. A Two-Machine System of a-c Generation of a Constant Frequency with a Variable Rotational Speed in the Drive. Trudy VVIA, No. 545, 1955.

Received Sept. 14, 1960.

DISTRIBUTION LIST

DEPARTMENT OF DEFENSE	Nr. Copies
HEADQUARTERS USAF	
AFCIN-3D2	1
ARL (ARB)	1
OTHER AGENCIES	
CIA	1
NSA	6
AID	2
OTS	2
AEC	2
PWS	1
NASA	1
RAND	1

MAJOR AIR COMMANDS	Nr. Copies
AFSC	
SCFTR	1
ASTIA	25
TD-Bla	5
TD-Blb	3
AEDC (AEY)	1
SSD (SSF)	2
BSD (BSF)	1
AFFTC (FTY)	1
AFSWC (SWF)	1
APGC (PGF)	1
ESD (ESY)	1
RADC (RAY)	1
AFMTC (MTW)	1